



UNIVERSIDADE FEDERAL DE GOIÁS  
FACULDADE DE ODONTOLOGIA  
PROGRAMA DE PÓS-GRADUAÇÃO EM ODONTOLOGIA

*RODRIGO ROCHA ANDRADE*

**INFLUÊNCIA DO TIPO E PROPORÇÃO DE PARTÍCULAS DE CARGA EM  
PROPRIEDADES MECÂNICAS DE UM COMPÓSITO EXPERIMENTAL**

Goiânia  
2015

**TERMO DE CIÊNCIA E DE AUTORIZAÇÃO PARA DISPONIBILIZAR AS TESES E DISSERTAÇÕES ELETRÔNICAS (TEDE) NA BIBLIOTECA DIGITAL DA UFG**

Na qualidade de titular dos direitos de autor, autorizo a Universidade Federal de Goiás (UFG) a disponibilizar, gratuitamente, por meio da Biblioteca Digital de Teses e Dissertações (BDTD/UFG), sem ressarcimento dos direitos autorais, de acordo com a Lei nº 9610/98, o documento conforme permissões assinaladas abaixo, para fins de leitura, impressão e/ou *download*, a título de divulgação da produção científica brasileira, a partir desta data.

**1. Identificação do material bibliográfico:**      **Dissertação**      **Tese**

**2. Identificação da Tese ou Dissertação**

Autor (a):	Rodrigo Rocha Andrade		
E-mail:	rodrigogoyaz@hotmail.com		
Seu e-mail pode ser disponibilizado na página?	<input checked="" type="checkbox"/> Sim	<input type="checkbox"/> Não	
Vínculo empregatício do autor			
Agência de fomento:		Sigla:	
País:	UF:	CNPJ:	
Título:	Influência da proporção de partículas de reforço nas propriedades mecânicas de um compósito experimental		
Palavras-chave:	Compósito reforçado com fibra; partícula de carga; matriz resinosa		
Título em outra língua:			
Palavras-chave em outra língua:	Influence of the ratio of reinforcement particles on the mechanical properties of a experimental composite I		
Área de concentração:	Clínica Odontológica		
Data defesa: (24/03/2015)			
Programa de Pós-Graduação:	Odontologia		
Orientador (a):	Rodrigo Borges Fonseca		
E-mail:	Rbfonseca.ufg@gmail.com		
Co-orientador (a):*			
E-mail:			

\*Necessita do CPF quando não constar no SisPG

**3. Informações de acesso ao documento:**

Concorda com a liberação total do documento  **SIM**      **NÃO**<sup>1</sup>

Havendo concordância com a disponibilização eletrônica, torna-se imprescindível o envio do(s) arquivo(s) em formato digital PDF ou DOC da tese ou dissertação.

O sistema da Biblioteca Digital de Teses e Dissertações garante aos autores, que os arquivos contendo eletronicamente as teses e ou dissertações, antes de sua disponibilização, receberão procedimentos de segurança, criptografia (para não permitir cópia e extração de conteúdo, permitindo apenas impressão fraca) usando o padrão do Acrobat.

*Rodrigo Rocha Andrade*

<sup>1</sup> Neste caso o documento será embargado por até um ano a partir da data de defesa. A extensão deste prazo suscita justificativa junto à coordenação do curso. Os dados do documento não serão disponibilizados durante o período de embargo.

***RODRIGO ROCHA ANDRADE***

**INFLUÊNCIA DO TIPO E PROPORÇÃO DE PARTÍCULAS DE CARGA EM  
PROPRIEDADES MECÂNICAS DE UM COMPÓSITO EXPERIMENTAL**

Dissertação apresentada ao Programa de Pós-Graduação em Odontologia da Faculdade de Odontologia da Universidade Federal de Goiás para obtenção do título de Mestre em Odontologia, área de concentração Clínica Odontológica.

Linha de Pesquisa: Avaliação do desempenho de materiais odontológicos

Orientador: Prof. Dr. Rodrigo Borges Fonseca

GOIÂNIA  
2015

Ficha catalográfica elaborada automaticamente  
com os dados fornecidos pelo(a) autor(a), sob orientação do Sibi/UFG.

Rocha Andrade, Rodrigo

Influência da proporção de partículas de reforço nas propriedades  
mecânicas de um compósito experimental [manuscrito] / Rodrigo Rocha  
Andrade. - 2015.  
56 f.: il.

Orientador: Prof. Dr. Rodrigo Borges Fonseca.  
Dissertação (Mestrado) - Universidade Federal de Goiás, Faculdade  
de Odontologia (FO), Programa de Pós-Graduação em Odontologia,  
Goiânia, 2015.  
Bibliografia. Anexos.  
Inclui gráfico, tabelas.

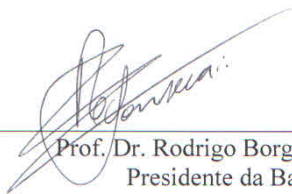
1. Compósito reforçado com fibra. 2. Partícula de carga. 3. Matriz  
resinosa. I. Borges Fonseca, Rodrigo, orient. II. Título.

---

## Rodrigo Rocha Andrade

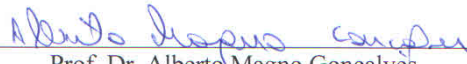
Influência da proporção de partículas de reforço nas propriedades mecânicas de um compósito experimental.

Dissertação defendida e aprovada em 24/03/2015, pela Banca Examinadora constituída por:



---

Prof. Dr. Rodrigo Borges Fonseca  
Presidente da Banca



---

Prof. Dr. Alberto Magno Gonçalves  
Membro da Banca



---

Prof. Dr. Rogério Vieira Reges  
Membro da Banca

## **DEDICATÓRIA**

Dedico este trabalho:

Ao meu orientador Prof. Dr. Rodrigo Borges Fonseca, por ser mais que um orientador, ser um amigo verdadeiro que me ensinou com muita paciência o caminho da docência. Gostaria que algum dia eu pudesse ser pelos menos um pouquinho do que ele é.

Aos meus pais Arnaldo e Nair, que sempre acreditaram em mim e me deram forças para continuar.

À minha esposa Nancy, por me servir de exemplo com sua disciplina e determinação em fazer tudo com perfeição e amor.

À minha filhinha Bianca, por ser meu amor incondicional e trazer tanta alegria para mim.

Aos meus irmãos Walter e Lugéria , aos meus cunhados Gilberto e Gilda, por sempre estarem presentes em todos os momentos da minha vida.

## **AGRADECIMENTOS**

À Universidade Federal de Goiás, à Faculdade de Odontologia e ao Programa de Pós-Graduação por me acolherem e proporcionar esta grandiosa oportunidade de aprendizado e crescimento profissional.

Aos meus queridos amigos de mestrado por terem me ensinado muito, tenho muito orgulho de todos vocês, sei que são excelentes profissionais e agora serão professores inesquecíveis.

À Amanda, Isabella, Letícia e Gustavo (Fiber Group) por terem me ajudado muito, serem companheiros sem nunca esperarem nada em troca.

Ao Prof. Dr. Rodrigo que me acolheu em seu grupo como um amigo sabendo driblar todas as minhas inúmeras dificuldades com muita paciência e compreensão.

Ao meu grande amigo Prof. Dr. Rogério Vieira Reges, por ser o meu grande incentivador na minha escolha profissional e acadêmica.

Ao Sr. Sérgio da Marconi Equipamentos Laboratoriais por gentilmente moer a fibra de vidro para a realização deste trabalho.

## RESUMO

Estudos prévios demonstram haver efetiva interação entre fibra de vidro silanizada e matriz resinosa formada por metacrilatos; porém, inexistente informação sobre a utilização da fibra de vidro moída e incorporada à resina como partícula de carga, com a finalidade de obter melhores propriedades mecânicas em compósitos destinados à fabricação de pinos intraradiculares. Os objetivos deste trabalho foram: avaliar a influência de diferentes tipos (silicato de bário e/ou pó de fibra de vidro) e concentrações de partícula de carga na resistência flexural, resistência à tração diametral e microdureza Knoop, de um compósito experimental composto por 47,5 % de partículas de carga, 30 % de fibra de vidro e 22,5 % de matriz resinosa (BISGMA e TEGDMA (1:1)); avaliar a morfologia das partículas de carga e sua interação com o compósito experimental em microscopia eletrônica de varredura. Para produção do pó de fibra de vidro, fibras foram moídas em um moinho almofariz/pistilo e então seis grupos experimentais (N = 10) foram confeccionados, variando a proporção do tipo de partícula de carga: CONTROLE – 47,5 % silicato de bário e 0,0 % pó de fibra de vidro; G7,5 – 40,0 % silicato de bário e 7,5 % pó de fibra de vidro; G17,5 – 30,0 % silicato de bário e 17,5 % pó de fibra de vidro; G27,5 – 20,0 % silicato de bário e 27,5 % pó de fibra de vidro; G37,5 % - 10,0 % silicato de bário e 37,5 % pó de fibra de vidro; G47,5 % - 0,0 % silicato de bário e 47,5 % pó de fibra de vidro. Amostras cilíndricas (3 mm x 6 mm) foram produzidas para o teste de resistência à tração diametral, e amostras em formato de barra (25 mm x 2 mm x 2 mm) para os testes de resistência flexural e microdureza Knoop. Os testes de resistência foram executados a 0,5 mm/min em máquina de ensaios universais (Instron 5965). O teste de microdureza Knoop foi feito a 0,2 KHN (200 g) por 40 segundos em um durômetro (HMV2 Shimadzu). Após verificação de normalidade e homogeneidade de distribuição dos dados com o teste Kolmogorov-Smirnov, os dados foram submetidos aos testes ANOVA e Tukey ( $\alpha=0,05$ ). Análises estatísticas demonstraram ( $p=0,001$ ): resistência flexural: CONTROLE -  $259,91\pm 26,01^a$ ; G7,5 -  $212,48\pm 35,91^b$ ; G17,5 -  $177,63\pm 24,88^{bc}$ ; G27,5 -  $166,58\pm 30,84^c$ ; G37,5 -  $92,08\pm 6,46^d$ ; G47,5 -  $80,60\pm 17,89^d$ ; Resistência à tração diametral: CONTROLE -  $31,05\pm 2,98^a$ ; G7,5 -  $14,55\pm 3,70^b$ ; G27,5 -  $12,65\pm 3,34^{bc}$ ; G17,5 -  $8,62\pm 3,51^{cd}$ ; G47,5 -  $8,04\pm 1,63^d$ ; G37,5 -  $6,63\pm 2,85^d$ ; Microdureza Knoop: CONTROLE -  $75,69\pm 12,19^a$ ; G37,5 -



67,62±1,79<sup>ab</sup>; G27,5 – 65,72±2,01<sup>b</sup>; G47,5 – 64,06±1,61<sup>b</sup>; G7,5 – 62,79±2,79<sup>b</sup>; G17,5 – 59,87±2,33<sup>b</sup>. A substituição gradativa em percentual do silicato de bário pelo pó de fibra de vidro em um compósito experimental reforçado com fibra de vidro resultou em queda nos resultados de resistência flexural, tração diametral e microdureza knoop. Morfologicamente, a partícula de pó de fibra de vidro apresentou-se heterogênea e com tamanho maior que a partícula do silicato de bário. A interação do pó de fibra de vidro com a matriz resinosa e o reforço de fibra não se mostraram efetivos.

Palavras-chave: Compósito reforçado com fibra. Partícula de carga. Matriz resinosa.

#### Abstract

Previous studies show that there is effective interaction between silanized glass fiber and resin matrix formed by methacrylates; However, there is no information on the use of milled glass fiber and the resin incorporated as a filler particle in order to obtain better mechanical properties in composites for the manufacture of intraradicular pins. The objectives of this study were to evaluate the influence of different types (barium silicate and / or glass fiber powder) and charged particle concentrations in flexural strength, resistance to diametrical and Knoop microhardness traction, an experimental composite composed of 47.5% loading of particles, 30 % glass fiber and resin matrix of 22.5% (BISGMA and TEGDMA (1: 1)); evaluate the morphology of the filler particles and their interaction with the experimental composite in scanning electron microscopy. For producing glass fiber powder, fibers were milled in a mortar grinder / pestle, and then six experimental groups (N = 10) were prepared, varying the ratio of the kind of charged particle: CONTROL - 47.5% barium silicate and 0.0% glass fiber powder; G7.5 - 40.0% barium silicate and 7.5% glass fiber powder; G17.5 - barium silicate 30.0% and 17.5% glass fiber powder; G27.5 - barium silicate 20.0% and 27.5% glass fiber powder; G37.5 - 10.0% barium silicate and 37.5% glass powder vibrates; G47.5% - 0.0% barium silicate and 47.5% glass fiber powder. Cylindrical samples (3 mm x 6

mm) were produced for the diametral tensile strength test, and samples in bar format (25 mm x 2 mm x 2 mm) for flexural and microhardness knoop throws. Resistance tests were performed at 0.5 mm / min on a universal testing machine (Instron 5965). The Knoop microhardness test was made 0.2 KHN (200 g) for 40 seconds at a hardness tester (Shimadzu HMV2). After verification of normality and homogeneity of data distribution with the Kolmogorov-Smirnov test, the data were submitted to ANOVA and Tukey tests ( $\alpha = 0.05$ ). Statistical analysis demonstrated ( $p = 0.001$ ): flexural strength: CONTROL -  $259.91 \pm 26.01^a$ ; G7.5 -  $212.48 \pm 35.91^b$ ; G17.5 -  $177.63 \pm 24.88^{bc}$ ; G27.5 -  $166.58 \pm 30.84^c$ ; G37.5 -  $92.08 \pm 6.46^d$ ; G47.5 -  $80.60 \pm 17.89^d$ ; Diametral tensile strength: CONTROL -  $31.05 \pm 2.98^a$ ; G7.5 -  $14.55 \pm 3.70^b$ ; G27.5 -  $12.65 \pm 3.34^{bc}$ ; G17.5 -  $8.62 \pm 3.51^{cd}$ ; G47.5 -  $8.04 \pm 1.63^d$ ; G37.5 -  $6.63 \pm 2.85^d$ ; Knoop microhardness: CONTROL -  $75.69 \pm 12.19^a$ ; G37.5 -  $67.62 \pm 1.79^{ab}$ ; G27.5 -  $65.72 \pm 2.01^b$ ; G47.5 -  $64.06 \pm 1.61^b$ ; G7.5 -  $62.79 \pm 2.79^b$ ; G17.5 -  $59.87 \pm 2.33^b$ . The gradual substitution a percentage of the barium silicate glass fiber powder in a glass fiber reinforced composite trial resulted in a decrease in the results of flexural strength, diametral tensile strength and Knoop hardness. Morphologically, glass fiber powder made up of particles with heterogeneous and larger than the particle of barium silicate. The interaction of the glass fiber powder to the resin matrix and fiber reinforcement have not proved effective.

Keywords: Fiber reinforced composite. Particle loading. Resin matrix.

## SUMÁRIO

1	INTRODUÇÃO .....	12
1.1	PROPOSIÇÃO .....	13
2	MATERIAL E MÉTODOS .....	14
2.1	GRUPOS EXPERIMENTAIS .....	15
2.2	MANIPULAÇÃO DO COMPÓSITO E GRUPOS EXPERIMENTAIS.....	16
2.3	CONFECÇÃO DAS AMOSTRAS .....	18
2.3.1	CONFECÇÃO DAS AMOSTRAS PARA TESTE DE RESISTÊNCIA À TRAÇÃO DIAMETRAL .....	18
2.3.2	CONFECÇÃO DAS AMOSTRAS PARA TESTE DE RESISTÊNCIA FLEXURAL .....	19
2.3.3	CONFECÇÃO DAS AMOSTRAS PARA TESTE DE DUREZA KNOOP .....	20
2.4	TESTES MECÂNICOS .....	21
2.4.1	TESTE DE RESISTÊNCIA À TRAÇÃO DIAMETRAL .....	21
2.4.2	TESTE DE RESISTÊNCIA FLEXURAL .....	22
2.4.3	TESTE DE MICRODUREZA KNOOP .....	23
2.5	MICROSCOPIA ELETRÔNICA DE VARREDURA .....	24
2.6	ANÁLISE ESTATÍSTICA .....	25
3	ARTIGO.....	26
4	CONSIDERAÇÕES FINAIS.....	43
5	REFERÊNCIAS.....	44
6	ANEXOS .....	47

## 1 INTRODUÇÃO

O desenvolvimento dos materiais odontológicos ampliou a utilização de restaurações em resina composta, um material polimérico com baixa resistência à tração [1]. Alguns desenvolvimentos deste material incluíram a associação à outros materiais, tais como: fibra de vidro, kevlar, carbono e polietileno de alto peso molecular [2, 3], com o objetivo de aumentar a resistência mecânica, com destaque maior para a fibra de vidro. A fibra de vidro pode ser usada como reforço dos polímeros odontológicos na confecção de pinos intraradiculares, próteses totais e coroas livres de metal de um a três elementos [4-9]. Em compósitos reforçados com fibra, alterações na quantidade, posição e tamanho das fibras adicionadas, além da associação de partículas de carga, altera as propriedades mecânicas do material [10-12].

Os compósitos reforçados com fibra podem apresentar propriedades mecânicas superiores às resinas convencionais reforçadas com partícula de carga [13]. Estudos demonstram melhora das propriedades mecânicas de resina composta associada à fibra de vidro [2, 5, 14-16]. A melhora nas propriedades dos compósitos reforçados por fibra de vidro é dependente de vários fatores: comprimento [17-19], orientação espacial [3, 4, 12, 13, 20], quantidade [18] e diâmetro [21] das fibras, adesão e impregnação da fibra pela matriz resinosa [2, 3, 21, 22], além do método de tratamento superficial das fibras [23].

Biomecanicamente, o uso das fibras associadas à compósitos resinosos apresenta como vantagem promover distribuição de tensões mais uniformes na estrutura dental, possibilitando a redução de fraturas catastróficas em dentes tratados endodonticamente [6]. Fibras de vidro de 3 mm de comprimento, aleatoriamente dispostas na matriz resinosa, têm resultado em altos valores de resistência devido à sua disposição multidirecional, o que proporciona reforço isotrópico aos materiais [17-19, 23, 24]. Garoushi *et al.* [24] utilizaram 22,5% em peso de fibra curta (3 mm de comprimento) com 55% em carga em 22,5% de matriz resinosa, e obtiveram uma resistência flexural de 210 MPa, maior que o grupo controle, sem fibra de reforço, que obteve 111 MPa de resistência flexural. Com o mesmo teste mecânico, Fonseca *et al.* [23] utilizam 30 % em peso da mesma fibra em 70 % de BISGMA e TEGDMA obtendo uma resistência 169,86 MPa. Porém, o material apresentou-se com alta

fluidez e difícil manipulação, o que gerou a hipótese de que seria necessário incluir partículas de carga para melhorar estas características.

As partículas de carga, assim como a fibra de vidro, melhoram as propriedades mecânicas dos compósitos e, a sua composição, dimensão, porcentagem em peso, morfologia e distribuição no material influenciam ainda na microdureza e na viscosidade da resina [1, 10, 11, 18, 25-37]. A adição de partículas de carga melhora a resistência flexural dos compósitos [25, 33]. Contudo, ao serem adicionadas sem tratamento superficial tem maior tendência a se aglomerarem ocasionando pontos de concentração de tensões e levando a falhas estruturais ou maior absorção de água que degrada a matriz resinosa [1]. A aplicação de silano, um agente de união, promove melhor interação entre partículas e resina [11]. O uso de partículas de carga com tamanho abaixo de 0,1  $\mu\text{m}$  possibilita melhorias mecânicas pela incorporação de grandes volumes de carga. Entretanto, existe grande dificuldade em silanizar e aderir à matriz resinosa partículas de tamanho muito reduzido devido a sua alta energia de superfície [36].

Pesquisas utilizam compósitos reforçados com fibra com frações em peso de fibra de vidro e partículas de carga de maneira variada [4, 6, 7, 9, 16, 20, 24, 29], buscando aliar suas propriedades mecânicas. Devido a adequada interação da fibra de vidro silanizada com matriz resinosa, especula-se que a produção de um pó de fibra de vidro e seu uso como partícula de carga poderia resultar em valores de resistência maiores. A melhora nas propriedades mecânicas desse compósito poderia favorecer a confecção de pinos intraradiculares ao mesmo tempo mais resistentes e biocompatíveis com a estrutura radicular, que é o intuito final de uma sequência de trabalhos da qual o presente estudo faz parte.

## 1.1 PROPOSIÇÃO

O presente estudo utilizou um compósito experimental[23] reforçado com 30% de fibra de vidro curta de 3mm em 22,5% de uma matriz resina a base de BISGMA e TEGDMA (1:1), manipulado com partículas de carga, com os objetivos de:

a) Avaliar a influência do tipo e proporção de partículas de carga (silicato de bário e ou pó de fibra de vidro) na resistência flexural, resistência à tração diametral e microdureza Knoop do material testado.

b) Avaliar a morfologia do pó de fibra de vidro em microscopia eletrônica de varredura.

c) Avaliar morfologicamente, por microscopia eletrônica de varredura, a associação entre a partícula de carga, fibra de vidro de reforço e matriz do compósito experimental.

## **2 MATERIAL E MÉTODOS**

### a) Tipo de estudo

Estudo laboratorial *in vitro*.

### b) Variáveis

Resistência Flexural, Resistência à Tração Diametral, Microdureza Knoop e Microscopia Eletrônica de Varredura.

### c) Fatores em Estudo

Tipo (pó de fibra de vidro e silicato de bário) e proporção de partículas de carga inseridas na resina experimental.

### d) Testes executados e materiais testados

Testes executados: Resistência Flexural de 3 pontos, Resistência à Tração Diametral, Microdureza Knoop e Microscopia Eletrônica de Varredura.

Materiais testados: BISGMA e TEGDMA (1:1); fibra de vidro curta (3 mm); silicato de bário e pó de fibra de vidro.

### e) Laboratório(s) utilizado(s)

Desenvolvido no laboratório de Biomecânica da Faculdade de Odontologia da Universidade Federal de Goiás, o qual não necessita de submissão ao Comitê de Ética em Pesquisa (CEP).

## 2.1 GRUPOS EXPERIMENTAIS

Seis grupos experimentais (N = 10) foram confeccionados pela inclusão de diferentes proporções de silicato de bário e pó da fibra de vidro (Tabela 1). A proporção de silicato de bário a 47,5 % foi obtida em estudo prévio [23], a partir dela, realizou-se a substituição gradativa pelo pó de fibra de vidro como partícula de carga.

**Tabela 1. Grupos Experimentais**

GRUPOS	PROPORÇÕES			
	% Fibra de vidro curta 3mm	% Resina	% Partícula de carga (silicato de bário)	% Partícula de carga (pó de fibra de vidro)
CONTROLE	30	22,5	47,5	0,0
G7,5	30	22,5	40,0	7,5
G17,5	30	22,5	30,0	17,5
G27,5	30	22,5	20,0	27,5
G37,5	30	22,5	10,0	37,5
G47,5	30	22,5	0,0	47,5

## 2.2 MANIPULAÇÃO DO COMPÓSITO E GRUPOS EXPERIMENTAIS

A resina utilizada teve como composição 50% 2,2-bis[4-(2 - hidróxi-3-metilacrilóxi)propóxi]fenil]-propano) (Bis-GMA , Sigma-Aldrich) e 50% dimetacrilato de trietilenoglicol (TEGDMA , Sigma-Aldrich), como sistema fotoiniciador 1 mol% de canforoquinona, 2 mol % de metacrilato de dimetilaminoetil (DMAEMA -, Sigma-Aldrich) e 0,1 mol % de hidroxitolueno butilado (BHT, Sigma-Aldrich), sendo esta manipulada em homogeneizador mecânico (Modelo ANS-000, SBS) (Figura 1).

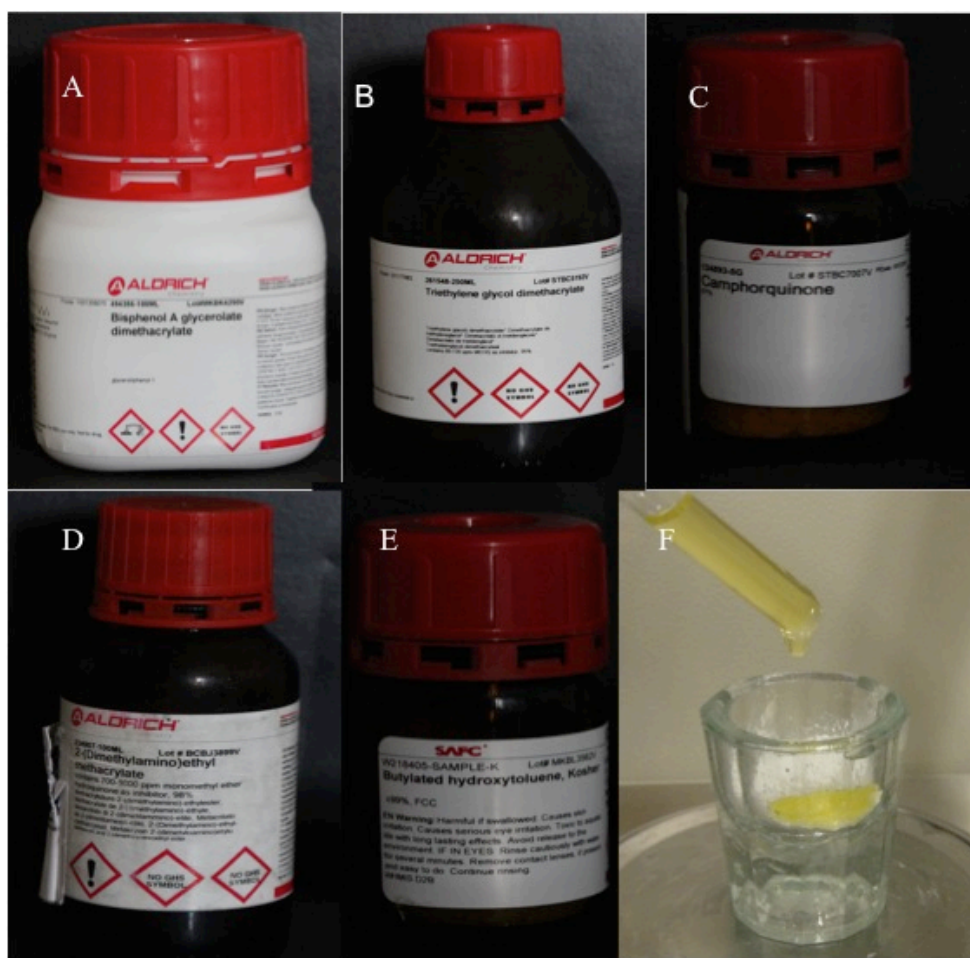


Figura 1. Materiais usados na manipulação do compósito: A – Bis-GMA; B – TEGDMA; C – Canforoquinona; D – DMAEMA; E – BHT; F – Resultado da manipulação dos materiais.

A partícula de carga obtida pelo pó de fibra de vidro (Figura 2A) foi produzida através da moagem (Moinho almofariz/pistilo – motorizado, marca Marconi, modelo MA 590 – Piracicaba – São Paulo – Brasil), com rotação de 50 rpm, por 1 hora e 30 minutos e a pressão aplicada não foi divulgada pelo fabricante do moinho. Logo após a moagem, esta foi silanizada e armazenada em local seco para evaporação dos



solventes. A partícula de silicato de bário (Figura 2B), com diâmetro médio de 0,7  $\mu\text{m}$  foi adquirida já pré-silanizada de fábrica (Esstech Inc., Essington, Pensilvânia, USA).



**Figura 2. Partículas de carga: A - Pó de fibra de vidro ; B – Silicato de bário**

A fibra de vidro de reforço utilizada no estudo, com corte industrial no comprimento de 3 mm (Owens Corning, Toledo, PR, Brasil), foi silanizada (Silano, Angelus, Londrina, PR, Brasil) e armazenada por 24 horas em ambiente seco para a evaporação dos solventes, antes de sua incorporação à resina com partícula de carga. A proporção de resina foi sempre de 22,5 % em peso e a de fibra de vidro de reforço foi de 30 % em peso.

A mistura de fibra na resina e a incorporação de partículas de carga (Figura 3), foram efetuadas manualmente após pesagem em balança analítica digital (AY220; Marte, Santa Rita do Sapucaí, Minas Gerais, BR) de acordo com os grupos experimentais. O compósito manipulado foi acondicionado em frasco de vidro âmbar e armazenado em ambiente livre de luz, para evitar a polimerização, sob refrigeração a 4° C.

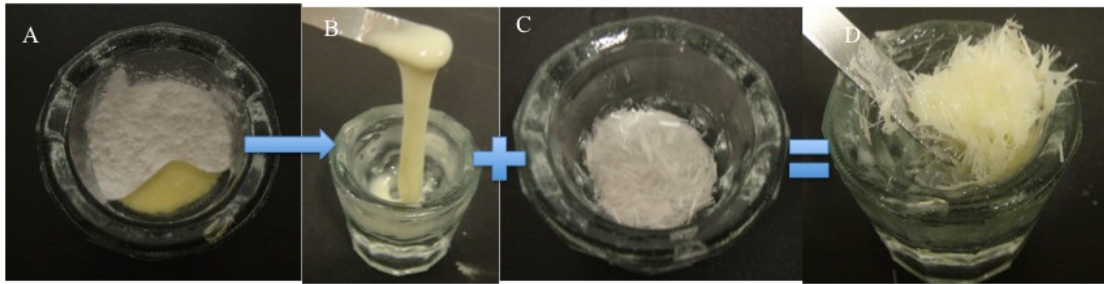


**Figura 3. Manipulação do compósito: A – Mistura do silicato de bário com a resina; B – Manipulação manual da resina com o silicato de bário; C - Fibra de vidro 3 mm de comprimento D – Manipulação manual do compósito com a fibra de vidro.**

### 2.3 CONFECÇÃO DAS AMOSTRAS

#### 2.3.1 CONFECÇÃO DAS AMOSTRAS PARA TESTE DE RESISTÊNCIA À TRAÇÃO DIAMETRAL

Dez amostras cilíndricas para cada grupo foram confeccionadas, a partir de uma matriz bipartida de alumínio, nas dimensões de 3,0 mm ( $\pm 0,1$ ) de altura por 6,0 mm ( $\pm 0,1$ ) de diâmetro, estando de acordo com a especificação da ADA n. 27[38]. O compósito foi inserido na matriz e sobreposto com tira de poliéster, sendo fotoativado por 40 segundos na face superior e inferior com 850 mW/cm<sup>2</sup> (Seasky; Tosi Foshan Medical Equipment Company, China). Em seguida as amostras foram removidas da matriz e polidas com lixas de carbeto de silício nas granulações 600 e 1200, em Lixadeira (TECLAGO, Vargem Grande, São Paulo, Brasil) com água corrente, por 10 s em cada face. Os corpos de prova foram então armazenados em água destilada, em estufa a 37° C, por 24 horas. Decorrido este período, as dimensões de cada corpo de prova foram conferidas, para verificar a padronização, com paquímetro digital (Mitutoyo, Tóquio, Japão), com precisão de 0,01 mm, e realizado o teste mecânico (Figura 4).

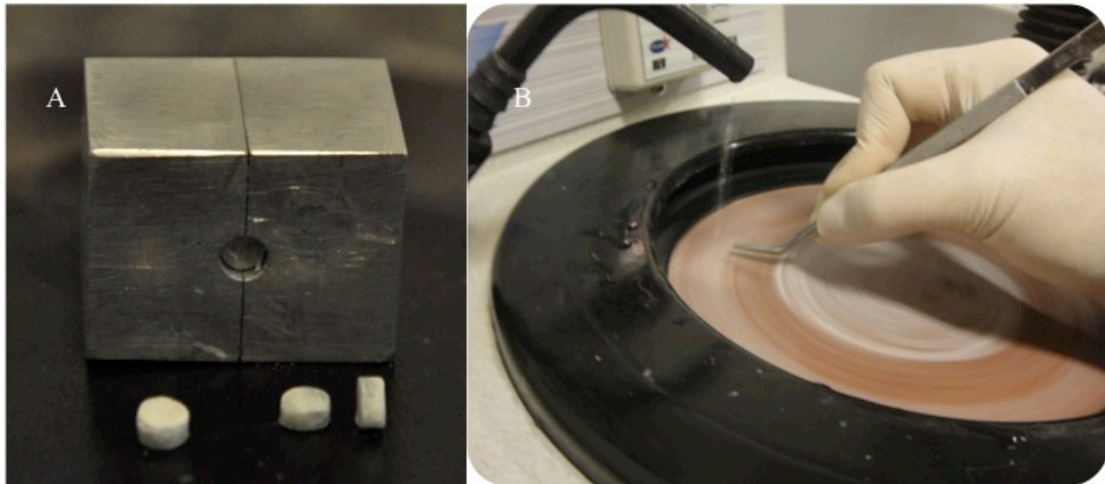


**Figura 4. Confeção das amostras do teste de resistência à tração diametral: A – Padrão de alumínio bipartido; B – Polimento da amostra em lixadeira.**

### 2.3.2 CONFEÇÃO DAS AMOSTRAS PARA TESTE DE RESISTÊNCIA FLEXURAL

Um molde de silicone (Clonage; Nova DFL, Jacarepaguá, Rio de Janeiro, BR) foi construído a partir de um padrão de alumínio a fim de permitir a confecção padronizada de dez amostras nas dimensões de 25 mm ( $\pm 2,0$ ) x 2 mm ( $\pm 0,1$ ) x 2 mm ( $\pm 0,1$ ), estando de acordo com a norma da ISO 4049/2000[39]. O compósito foi inserido no molde e sobreposto com tira de poliéster. Logo após foi realizada a fotoativação por 40 segundos na face superior com 850 mw/cm<sup>2</sup> (Seasky; Tosi Foshan Medical Equipament Company, Foshan, Guangdong, China).

Após a confecção das amostras, estas sofreram o mesmo processo de polimento, armazenamento e aferição de tamanho das amostras do teste anterior, seguindo-se o teste mecânico (Figura 5).

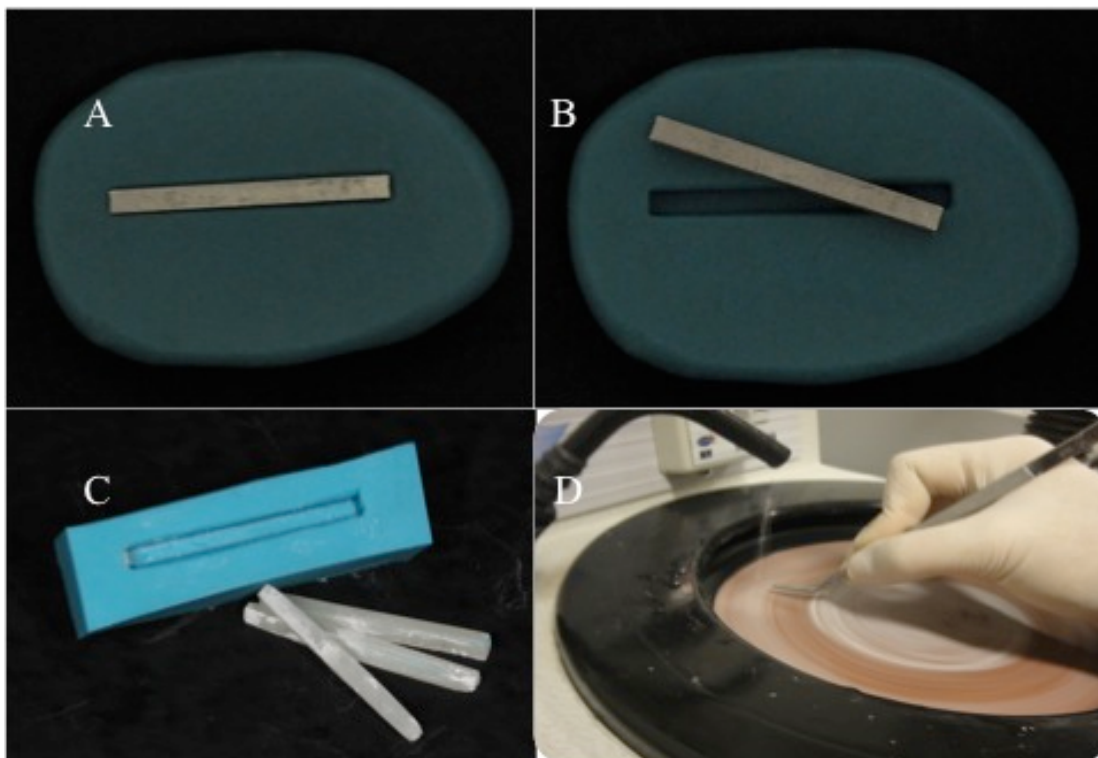


**Figura 5. Confeção das amostras do teste de resistência flexural: A – Padrão de alumínio incluído em silicona de condensação; B – Molde de silicona de condensação; C – Amostras padronizadas para o teste de resistência flexural; D – Polimento da amostra em lixadeira.**

### 2.3.3 CONFECÇÃO DAS AMOSTRAS PARA TESTE DE DUREZA KNOOP

Para avaliação da dureza do compósito experimental, foram confeccionadas cinco amostras de cada grupo experimental, um total de trinta, nas dimensões de 25 mm ( $\pm 2,0$ ) x 2 mm ( $\pm 0,1$ ) x 2 mm ( $\pm 0,1$ ), seguindo o mesmo protocolo descrito para as amostras submetidas ao teste de resistência flexural. Decorrido o período de armazenagem em água destilada a 37° C por 24 horas, as amostras foram incluídas em resina de poliestireno para a realização do teste de resistência à penetração por microdureza knoop. Nesta etapa, um cilindro de PVC foi posicionado e fixado com cera em torno das amostras, e resina de poliestireno autopolimerizável (Cristal; Araquímica, Araçariguama, São Paulo, Brasil) foi manipulada e vertida no interior do cilindro de PVC. Decorridas 2 horas da inclusão, o conjunto foi retirado da placa de suporte e foi realizado o acabamento com lixas de carbetto de silício nas granulações 600, 1200 e 2000 em Lixadeira (TECLAGO) com água corrente até a obtenção de

uma superfície visualmente lisa e uniforme, e logo em seguida foi realizado o teste mecânico (Figura 6).

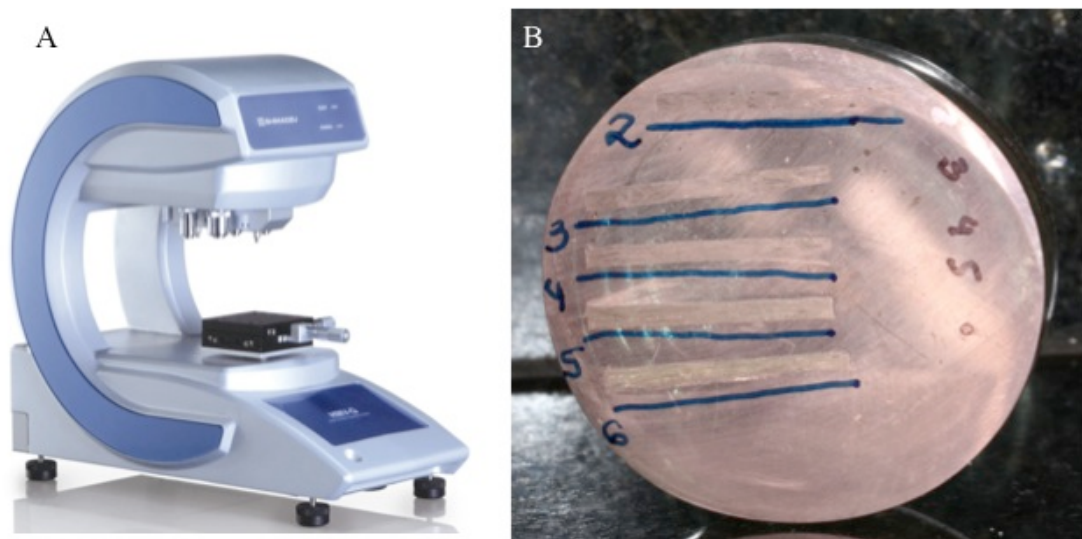


**Figura 6. Teste de microdureza knoop: A – Microdurometro (Fonte: Shimadzu); B – Corpo de prova para teste em microdurometro.**

## 2.4 TESTES MECÂNICOS

### 2.4.1 TESTE DE RESISTÊNCIA À TRAÇÃO DIAMETRAL

Para o teste de resistência à tração diametral, as amostras foram posicionadas em máquina de ensaio universal (Instron 5965, Instron Corporation, Norwood, Minnesota, EUA). Uma carga compressiva a velocidade constante de 0,5 mm/min foi aplicada na superfície diametral das amostras até sua ruptura, sendo a carga máxima registrada em N. A resistência a tração diametral de cada amostra foi obtida, em MPa, de acordo com a seguinte fórmula:

$f = 2F / \pi dL$  onde “f” é a resistência à tração por compressão diametral, “F” é carga máxima obtida no ensaio (KgF), “d” é o diâmetro do corpo de prova (6,0 mm) e “L” a altura (3,0 mm) (Figura 7).

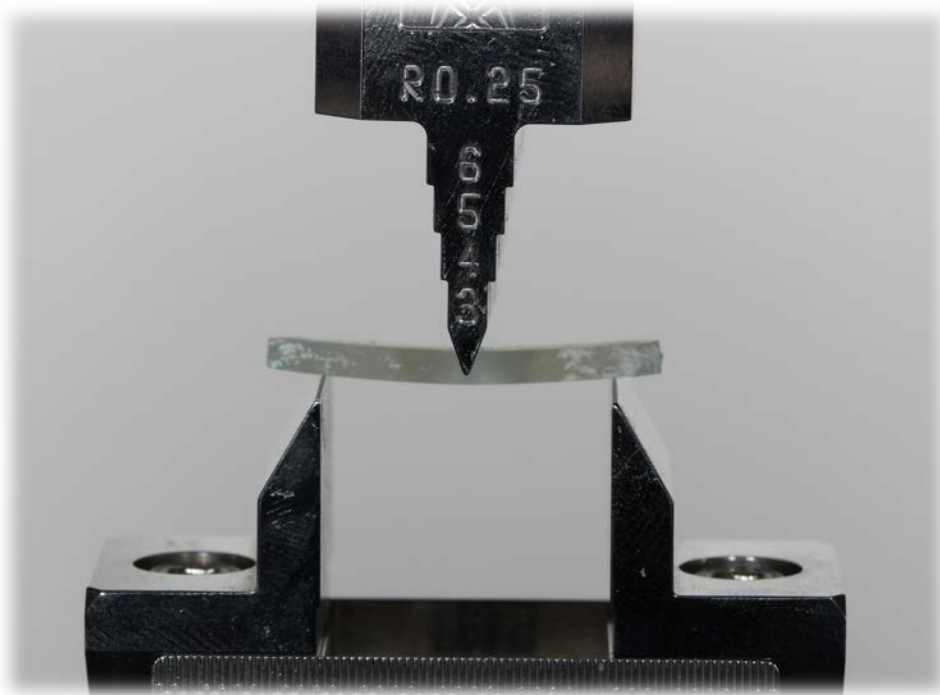


Figura 7. Teste de resistência à tração diametral (Instron).

#### 2.4.2 TESTE DE RESISTÊNCIA FLEXURAL

O teste de resistência flexural de três pontos foi realizado em máquina de ensaio universal (Instron 5965), sendo a amostra posicionada sobre dois pontos com 20 mm de distância entre si e equidistantes do centro. Um ponto central de aplicação de carga foi definido. Foi aplicada uma carga a velocidade constante de 0,5 mm/min e a carga máxima à fratura registrada em Newton (N). A Resistência Flexural (RF) de cada amostra foi obtida, em MPa, de acordo com as seguinte fórmula:

$RF = 3 \cdot P \cdot L / 2 \cdot w \cdot b^2$  onde “P” é a carga máxima aplicada até a fratura, “L” é a distância entre os apoios (20 mm), “w” é a espessura da amostra (2,0 mm) e “b” a altura (2,0 mm), “F” é a força aplicada em uma porção reta linear do gráfico tensão-deformação, “d” é a correspondente deformação originada por esta força (Figura 8).



**Figura 8. Teste de resistência flexural.**

#### 2.4.3 TESTE DE MICRODUREZA KNOOP

Cinco penetrações foram efetuadas em cada superfície com durômetro (HMV2; Shimadzu, Tóquio, JP) com carga de 200 g por 40 s. A média das penetrações para cada superfície foi registrada como o número de microdureza Knoop (KHN) (Figura 9).

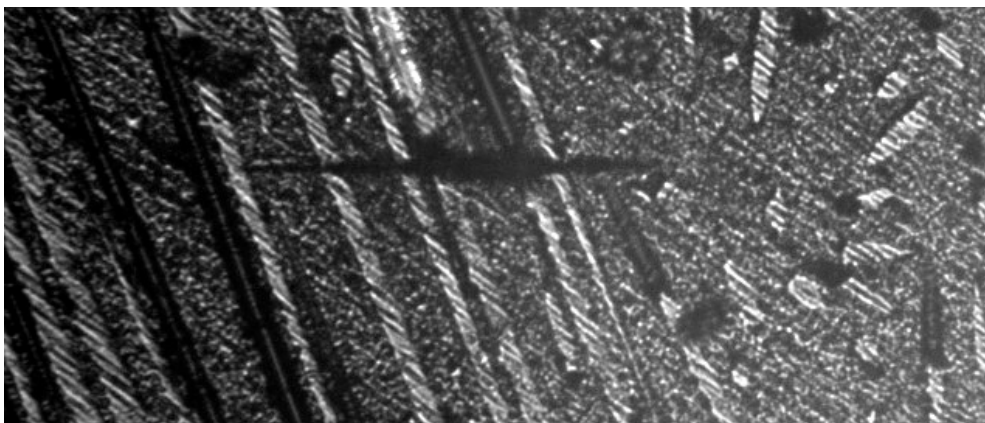


**Figura 9. Teste de dureza knoop: A – Indentação em uma das amostra do grupo G7,5.**

## 2.5 MICROSCOPIA ELETRÔNICA DE VARREDURA

Para análise em microscopia eletrônica de varredura (MEV), foram selecionadas 2 amostras aleatórias de cada grupo fraturadas durante o teste de resistência à flexão e 2 amostras íntegras. Também foi selecionada uma pequena quantidade de silicato de bário e pó de fibra de vidro. As amostras foram fixadas em *stubs* metálicos e posicionadas no metalizador (Denton Vacuum; Desk V, Moorestown, New Jersey, EUA), para deposição superficial de fina camada de carbono. Após a metalização, as amostras foram examinadas em MEV de pressão variável, em alto vácuo (Jeol; JSM – 6610, equipado com EDS, Thermo scientific NSS Spectral Imaging. São Paulo, São Paulo, Brasil), focalizando-se e analisando as características morfológicas e a concentração das partículas de carga e sua interação com a fibra de vidro e a matriz resinosa (Figura 10).

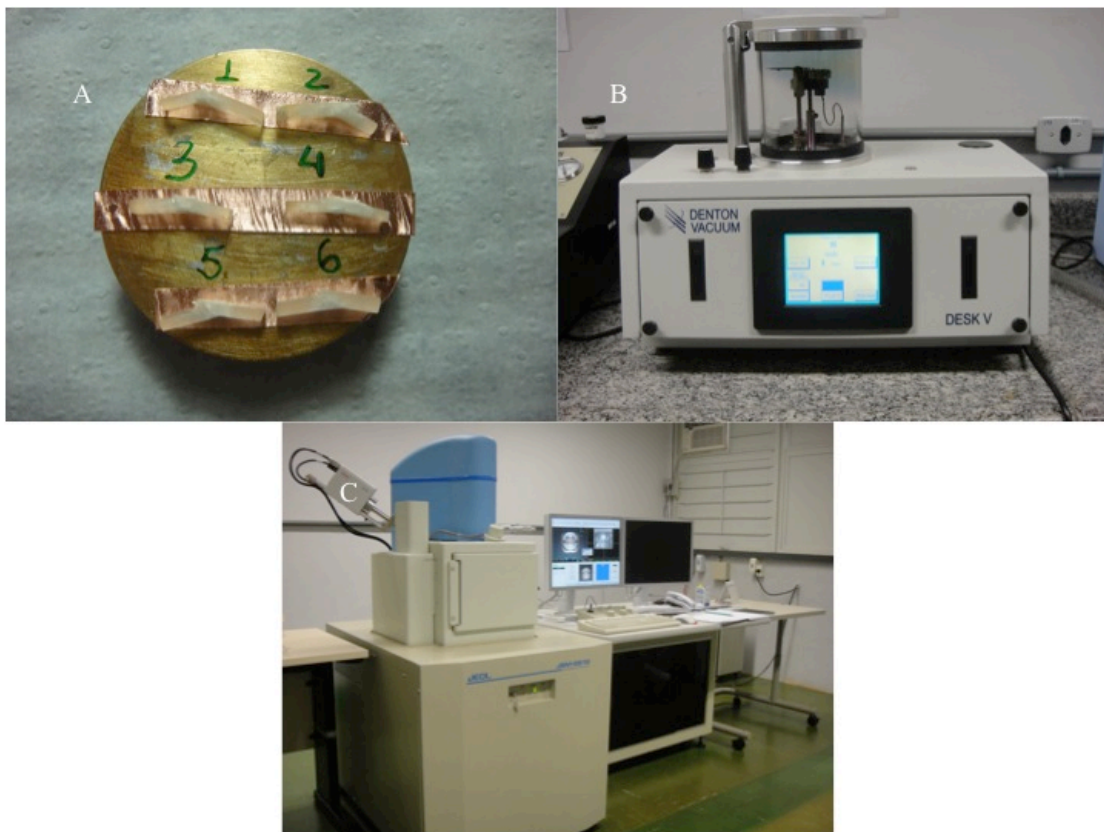


**Figura 10. Microscopia eletrônica de varredura: A – Amostras dos seis grupos de resistência flexural em stbs; B – Metalizador Denton Vacuum; C - Microscópio eletrônico de varredura JSM 6610.**



## 2.6 ANÁLISE ESTATÍSTICA

Os dados foram analisados pelo teste de Kolmogorov-Smirnov para verificar a normalidade e homogeneidade de distribuição e posteriormente analisados pelos testes Anova e Tukey para comparações entre grupos. Todos os testes foram realizados ao nível de significância de 5 % no programa SPSS20.0 (SPSS, Chicago, EUA).

### 3 ARTIGO

#### MECHANICAL PROPERTIES OF A REINFORCED METHACRYLATE AFTER ADDITION OF GLASS FIBER POWDER

Rodrigo R. Andrade<sup>1</sup>, Amanda V. B. Kasuya<sup>2</sup>, Isabella N. Favarão<sup>2</sup>, Leticia N. de Almeida<sup>1</sup>, Gustavo A. M. Mendes<sup>1</sup>, Rodrigo B. Fonseca<sup>3</sup>.

1 - Mestrando do Departamento de Dentística Restauradora, Faculdade de Odontologia da Universidade Federal de Goiás, Goiânia, Goiás, Brasil.

2 - Doutorando do Departamento de Dentística Restauradora, Faculdade de Odontologia da Universidade Federal de Goiás, Goiânia, Goiás, Brasil.

3 – Professor Doutor do Departamento de Dentística Restauradora, Faculdade de Odontologia da Universidade Federal de Goiás, Goiânia, Goiás, Brasil.

Autor Correspondente: Rodrigo Borges Fonseca Dentistry School, UFG, 1a. Avenida esquina com Praça Universitária, s/n, Faculdade de Odontologia, Setor Universitário - CEP 74.605-220 Goiânia-GO, Brazil. Telefone: 55 62 3209 6050 Fax: 55 62 3521 1882

[rbfonseca.ufg@gmail.com](mailto:rbfonseca.ufg@gmail.com)

## MECHANICAL PROPERTIES OF A REINFORCED METHACRILATE AFTER ADDITION OF GLASS FIBER POWDER

### Abstract

Previous studies show that there is effective interaction between silanized glass fiber and resin matrix formed by methacrylates; However, there is no information on the use of milled glass fiber and the resin incorporated as a filler particle in order to obtain better mechanical properties in composites for the manufacture of intraradicular pins. The objectives of this study were to evaluate the influence of different types (barium silicate and / or glass fiber powder) and charged particle concentrations in flexural strength, resistance to diametrical and Knoop microhardness traction, an experimental composite composed of 47.5% loading of particles, 30 % glass fiber and resin matrix of 22.5% (BISGMA and TEGDMA (1: 1)); evaluate the morphology of the filler particles and their interaction with the experimental composite in scanning electron microscopy. For producing glass fiber powder, fibers were milled in a mortar grinder / pestle, and then six experimental groups (N = 10) were prepared, varying the ratio of the kind of charged particle: CONTROL - 47.5% barium silicate and 0.0% glass fiber powder; G7.5 - 40.0% barium silicate and 7.5% glass fiber powder; G17.5 - barium silicate 30.0% and 17.5% glass fiber powder; G27.5 - barium silicate 20.0% and 27.5% glass fiber powder; G37.5 - 10.0% barium silicate and 37.5% glass powder vibrates; G47.5% - 0.0% barium silicate and 47.5% glass fiber powder. Cylindrical samples (3 mm x 6 mm) were produced for the diametral tensile strength test, and samples in bar format (25 mm x 2 mm x 2 mm) for flexural and microhardness Knoop throws. Resistance tests were performed at 0.5 mm / min on a universal testing machine (Instron 5965). The Knoop microhardness test was made 0.2 KHN (200 g) for 40 seconds at a hardness tester (Shimadzu HMV2). After verification of normality and homogeneity of data distribution with the Kolmogorov-Smirnov test, the data were submitted to ANOVA and Tukey tests ( $\alpha = 0.05$ ). Statistical analysis demonstrated ( $p = 0.001$ ): flexural strength: CONTROL -  $259.91 \pm 26.01^a$ ; G7.5 -  $212.48 \pm 35.91^b$ ; G17.5 -

$177.63 \pm 24.88^{bc}$ ; G27.5 -  $166.58 \pm 30.84^c$ ; G37.5 -  $92.08 \pm 6.46^d$ ; G47.5 -  $80.60 \pm 17.89^d$ ; Diametral tensile strength: CONTROL -  $31.05 \pm 2.98^a$ ; G7.5 -  $14.55 \pm 3.70^b$ ; G27.5 -  $12.65 \pm 3.34^{bc}$ ; G17.5 -  $8.62 \pm 3.51^{cd}$ ; G47.5 -  $8.04 \pm 1.63^d$ ; G37.5 -  $6.63 \pm 2.85^d$ ; Knoop microhardness: CONTROL -  $75.69 \pm 12.19^a$ ; G37.5 -  $67.62 \pm 1.79^{ab}$ ; G27.5 -  $65.72 \pm 2.01^b$ ; G47.5 -  $64.06 \pm 1.61^b$ ; G7.5 -  $62.79 \pm 2.79^b$ ; G17.5 -  $59.87 \pm 2.33^b$ . The gradual substitution a percentage of the barium silicate glass fiber powder in a glass fiber reinforced composite trial resulted in a decrease in the results of flexural strength, diametral tensile strength and Knoop hardness. Morphologically, glass fiber powder made up of particles with heterogeneous and larger than the particle of barium silicate. The interaction of the glass fiber powder to the resin matrix and fiber reinforcement have not proved effective.

Keywords: Fiber. Composite. Particle. Scanning electron microscopy

## 1 INTRODUCTION

The development of dental materials has expanded the use of composite resin restorations, a polymeric material with low tensile strength [1]. Some of this material developments have included combination with other materials, such as fiberglass, Kevlar, carbon and high molecular weight polyethylene [2, 3], in order to increase the mechanical strength, most notably fiberglass. The glass fiber can be used as reinforcement of polymer in the manufacture of dental intraradicular pins, dentures and a metal free crowns three elements [4-9]. In fiber reinforced composites, changes in the quantity, position and size of added fiber, and the filler particles association change the mechanical properties [10-12].

The composites reinforced with fiber may have superior mechanical properties to conventional resins reinforced with filler particle [13]. Studies show improved mechanical properties of composite associated with glass fiber [2, 5, 14-16]. The improved properties of composites reinforced by glass fiber is dependent upon several factors: length [17-19], spatial orientation [3, 4, 12, 13, 20], number [18] and diameter [21] of the fibers, adhesion and impregnation of the fiber resin matrix [2, 3, 21, 22] as well as the surface treatment method for fiber [23].

Biomechanically, the use of fibers attached to the resin composite has the advantage of promoting more uniform distribution of stresses in the tooth structure, enabling reduction of catastrophic fracture of endodontically treated teeth [6]. Glass fibers of 3 mm long, randomly arranged in the resin matrix, have resulted in higher resistance values due to their multidirectional array, which provides enhanced isotropic materials [17-19, 23, 24]. Garoushi et al. [24] used 22.5% short fiber weight (3 mm long) with 55% load in 22.5% of resin matrix, and obtained a flexural strength of 210 MPa, higher than the control group without fiber reinforcement, which obtained 111 MPa of flexural strength. With the same mechanical testing, Fonseca et al. [23] using 30% by weight of the same fiber in 70% yield BISGMA and TEGDMA 169.86 MPa resistance. However, the material presented with high fluidity and difficult to handle, which led to the hypothesis that would need to include filler particles to improve these characteristics.

The filler particles as well as glass fiber, improve the mechanical properties of the composites and their composition, size, percentage by weight, morphology and

distribution in the material also influence the hardness and viscosity of the resin [1, 10, 11, 18, 25-37]. The addition of filler particles improves the flexural strength of the composite [25, 33]. However, when added without surface treatment has a greater tendency to agglomerate causing stress concentration points, and structural failure leading to increased water absorption or that degrades resin matrix [1]. The application of silane, a coupling agent, promotes better interaction between particles and resin [11]. The use of filler particles with a size below 0.1 microns enables mechanical improvements by incorporating large volumes of goods. However, there is great difficulty in silanize and adhere to the matrix resin very small particle size due to its high surface energy [36]

Searches using fiber reinforced composites with glass fiber fractions in weight and filler particles variously [4, 6, 7, 9, 16, 20, 24, 29], in order to combine their mechanical properties. Due to proper interaction of silanized glass fiber resin matrix, it is speculated that the production of a glass fiber powder and its use as a filler particle would result in higher resistance values. The improvement in the mechanical properties of the composite could favor the production of intraradicular pins while more resistant and biocompatible with the root structure, which is the final purpose of a sequence of jobs which this part of the study.

The present study used an experimental reinforced composite made by 30% 3mm-short glass fiber in 22.5% resin matrix (BISGMA and TEGDMA, 1: 1) with the following aims:

a) to evaluate the influence of type and filler loading ratio (barium silicate glass fiber or glass fiber powder) on the mechanical strength (flexural and diametral tensile strength) and Knoop microhardness.

b) to assess the morphology of glass fiber powder by scanning electron microscopy (SEM).

c) to evaluate by the association between the fillers, reinforcing glass fiber and resin matrix of experimental composite by SEM.

## 2 MATERIAL AND METHODS

### 2.1 EXPERIMENTAL GROUPS

Six experimental groups (N = 10) were prepared by adding different proportions of barium silicate, and glass fiber powder(GFP) (Table 1). The proportion of barium silicate 47.5% was obtained in a previous study [23], as it was held by the gradual replacement of GFP as a filler particle.

### 2.2 MANIPULATION OF COMPOSITE EXPERIMENTAL AND EXPERIMENTAL GROUPS

The charged particle obtained by GFP was produced by grinding (mill mortar / pestle - motorized Marconi brand, model MA 590 - Piracicaba - Sao Paulo - Brazil), with a rotation of 50 rpm for 1 hour 30 minutes and the applied pressure was not released by the mill manufacturer. Immediately after grinding, it was silanized and stored in dry place for evaporation of the solvents. The barium silicate particle with a mean diameter of 0.7 microns has been acquired pre-silanized plant (Esstech Inc., Essington, Pennsylvania, USA).

The reinforcing glass fiber used in the study, with industrial cutting the length of 3 mm (Owens Corning, Toledo, PR, Brazil) was silanized (Silane, Angelus, Londrina, PR, Brazil) and stored for 24 hours in dry conditions for evaporation of the solvents, prior to its merger with the resin particle of charge. The proportion of resin was always 22.5% by weight and the reinforcing glass fiber was 30% by weight.

The fiber blend in the resin and the incorporation of charged particles, were made manually after weighing in digital analytical balance (AY220, Mars, Santa Rita do Sapucaí, Minas Gerais, BR) according to the experimental groups. The engineered composite was packed in amber glass vial and stored in light-free environment to prevent polymerization under refrigeration at 4 ° C.

### 2.3 DIAMETRAL TENSILE STRENGTH TEST

Ten cylindrical samples for each group were made from an aluminum metallic mold, the dimensions of 3.0 mm ( $\pm 1.0$ ) mm high and 6.0 ( $\pm 1.0$ ) diameter, which is consistent specifying the ADA n. 27. [38] The composite was inserted into the array and overlapped with polyester strip, and light cured for 40 seconds on the upper side and lower with 850 mW / cm<sup>2</sup> (Seasky; Tosi Foshan Medical Equipament Company, China). Then the samples were removed from the matrix and polished with sandpaper silicon carbide granules in 600 and 1200, in Sander (TECLAGO - Vargem Grande - Sao Paulo - Brazil) with running water for 10 seconds on each side. The samples were then stored in distilled water in an oven at 37 C for 24 hours. After this period, the dimensions of each specimen were checked to verify the standardization, with a digital caliper (Mitutoyo, Tokyo, Japan) with a precision of 0.01 mm.

For diametral tensile strength test, the samples were placed in a universal testing machine (Instron 5965, Instron Corporation, Norwood, Minnesota, USA). A constant compressive load rate of 0.5 mm / min was applied to the diametrical surface of the samples to burst, with the maximum load recorded N. The diametral tensile strength of each sample was obtained in MPa

### 2.4 FLEXURAL STRENGTH TEST

A silicone mold (Cloning; New DFL, the studied area, Rio de Janeiro BR) was constructed from an aluminum standard to allow the standardized manufacture of the ten samples of dimensions 25 mm ( $\pm 2.0$ ) x 2 mm ( $\pm 0.1$ ) x 2 mm ( $\pm 0.1$ ), which is consistent with the ISO standard 4049/2000. [39] the composite was inserted into the mold and overlaid with a polyester strip. Soon after the polymerization was carried out for 40 seconds on the upper surface with 850 mw / cm<sup>2</sup> (Seasky; Tosi Foshan Medical Equipament Company, Foshan, Guangdong, China).

The flexural strength test was conducted three points on a universal testing machine (Instron 5965), and the sample positioned on two points 20 mm apart from each other and equidistant from the center. A central point load application has been set. Was applied a load at a constant speed of 0.5 mm / min and the maximum load to



fracture recorded in Newton (N). The flexural strength (RF) of each sample was obtained in MPa.

## 2.5 KNOOP MICROHARDNESS TEST

For experimental evaluation of microhardness composite, five samples were prepared for each experimental group a total of thirty, the dimensions of 25 mm ( $\pm 0.2$ ) x 2 mm ( $\pm 0.1$ ) x 2 mm ( $\pm 0.1$ ) following the same protocol described for the samples subjected to bending strength test. After the period of storage in distilled water at 37 ° C for 24 hours, the samples were embedded in polystyrene resin for holding the penetration resistance test - Knoop microhardness. In this step, a PVC cylinder was positioned and secured with wax around the samples, and self-curing resin polystyrene (Crystal; Araquímica, Araçariguama, São Paulo, Brazil) has been manipulated and poured into the PVC cylinder. After 2 hours the addition, the whole was removed from the support plate and finishing was carried out with silicon carbide abrasives in grits 600, 1200 and 2000 sander with water to obtain a smooth and uniform surface.

For the hardness test, five indentations were made on each surface microhardness (HMV2; Shimadzu, Tokyo, Japan) with 200 g load for 40 s. The average indentations for each surface was recorded as the number of Knoop hardness (KHN).

## 2.6 SCANNING ELECTRON MICROSCOPY

For analysis in scanning electron microscopy (SEM), we selected two random samples of each group fractured during the flexural strength test and two intact samples. It was also selected a small amount of barium silicate and GFP. The samples were fixed on metal stubs and sputter positioned at (Denton Vacuum, Desk V, Moorestown, New Jersey, USA) for surface deposition of thin carbon layer. After plating, the samples were examined in variable pressure SEM in high vacuum (Jeol; JSM - 6610, equipped with EDS, Thermo scientific NSS Spectral Imaging São Paulo, São Paulo, Brazil), focusing up and analyzing the characteristics morphological and the percentage concentration of filler particles and their interaction with the glass fiber and the resin matrix.

## 2.7 STATISTICAL ANALYSIS

The data were analyzed using the Kolmogorov-Smirnov test to verify the normality and homogeneity of distribution and subsequently analyzed by ANOVA and Tukey test for comparisons between groups. All tests were performed at the 5% significance level SPSS20.0 (SPSS, Chicago, USA).

## 3 RESULTS

### 3.1 DIAMETRAL TENSILE STRENGTH

The result of the diametral tensile test showed a significant reduction in resistance as the addition of GFP was performed as charged particle ( $p < 0.05$ ). The average resistance ranged from 31.05 to 6.62 MPa and the highest resistance value was obtained for the control group had 0% GFP. The G7.5 group had the second best result of the diametral tensile strength, however this was statistically similar to G27.5 group. The other groups, G17.5, G37.5 and G47.5, statistically lower (Figure 1).

### 3.2 FLEXURAL STRENGTH

Similarly, as observed for diametral tensile results, the results of the flexural resistance test showed a significant reduction of resistance in accordance with the gradual addition was made of GFP as a filler particle. The average variation in flexural strength between the groups was 259, from 91 to 80.6 MPa. CONTROL group had the highest average flexural strength and was statistically different from the other groups. The G7.5 and G17.5 groups were statistically similar results below the CONTROL group, followed by G27.5 group. The G37.5 and G47.5 groups had the lowest averages were statistically similar (Figure 2).

### 3.3 KNOOP MICROHARDNESS

The results of Knoop hardness test showed a decrease in hardness as the addition of GFP was performed as filler particle. The average hardness variation between groups was 75.69 to 64.06 KHN. CONTROL group had the highest average knoop hardness, statistically similar to G37.5, and all other below the CONTROL and similar to G37.5 (FIGURE 3).

### 3.4 SCANNING ELECTRON MICROSCOPY

For the analysis of scanning electron microscopy, images of the particles of fiberglass powder showed morphologically heterogeneous material, with varying length and diameter similar to the reinforcing fiber, which was  $\pm 14$  microns (Figure 4 A and B) . In turn, the particles of barium silicate filler proved to be more homogeneous (Fig 4 C and D).

The control group showed a homogeneous images resin matrix adhered to the reinforcing fibers, without the presence of bubbles and cracks (Figure 5), demonstrating the good interaction of the reinforcing fibers resinous matrix, in addition to the effective incorporation of the silicate filler particles barium the resin matrix. The images of G7.5 group had bubbles and spaces with no reinforcing fibers which could be observed crack propagation. Fiberglass dust load Incorporation of 7.5% resulted in a homogeneous particle array (Figure 6).

For G17.5 group can be observed the presence of cracks and bubbles associated with a region where there was no reinforcement fibers (Figure 7). At increasing 330 x (Figure 7 B) was observed to crack propagation by the bubble and a homogeneous resin matrix.

The G27.5 group in its microscopy showed a heterogeneous resin matrix groups with single GFP filler particles in the absence of reinforcement fiber bundles (Figure 8). At increasing 650 x (Figure 8B) showed that the glass fiber bundles powder spread in various directions, demonstrating the difficulty of incorporation of 27.5% GFP particle loading, besides the interaction inability of such particle with the resin matrix when used in larger amounts.

The experimental group G37.5 had in their microscopic areas with large GFP agglomerates, in the presence of multidirectional reinforcement beam attached to the glass fibers a mixed resin matrix (Figure 9), which also observed no reinforcing fibers and bubbles at certain points (Figure 9b).

The microscopy G47.5 group showed several areas with clusters of powdered glass fiber bundles, multi-directional, with no reinforcing fiber (Figure 10 A and B). Showed areas with fiber reinforcement beams with low adhesion to the resin matrix interspersed with GFP agglomerates (Figure 10 C and D). There was a slightly heterogeneous resin matrix adhered to the GFP (Figure 10 E).

#### 4 DISCUSSION

This study examined the influence of type and filler loading ratio (barium silicate glass fiber or powder) in flexural strength and diametral tensile strength and Knoop hardness of an experimental resin containing 30% of 3mm-short glass fiber in 22.5% resinous matrix (BISGMA and TEGDMA, 1: 1). Since the use of silanized glass fiber enhances the strength of composites [2, 4-7, 9, 12-14, 17, 21, 23, 24, 40, 41] this study hypothesized that the incorporation fiber powder glass as a filler particle could increase mechanical properties.

However, the gradual replacement of a traditional filler particle, barium silicate, by GFP did not show the expected result, since diametral tensile strength, flexural strength and Knoop microhardness results were lower than control group. The present results showed an increase in mechanical fragility of the specimens; experimental groups with higher concentrations of GFP showed an heterogeneous resin matrix with irregular distribution of the reinforcing fibers, leading to formation of internal voids.

SEM analysis of barium silicate fillers showed uniform particle size, as specified by the manufacturer (0.7  $\mu\text{m}$ ). Small filler diameters tends to increase mechanical strength of composites [1, 25-27, 29, 34]. Increased strength is also influenced by filler silanization [30]. After silanized, greater amounts of fillers can be inserted in a resin matrix, and then the GFP was silanized before incorporation into the resin matrix. However, GFP microscopy (Figure 3) showed that the milling procedure was not enough to produce an homogeneous powder, resulting in particles with different sizes and same diameters of the traditional reinforcing glass fibers. The initial aim was to obtain glass powder fillers with an average size less than or equal to 0.7  $\mu\text{m}$  (barium silicate filler size); however, some GFP fillers exceeded 144  $\mu\text{m}$  (Figure 4), which probably hindered its action as filler particles. On the other hand, they could operate as true reinforcing fibers but measured length was less than the critical length required to exert this effect, which is 1.5 mm [18, 19]. Since the diameter of GFP was similar to the one of reinforcing fibers, the fillers occupied some sites of glass fibers, decreasing the mechanical strength of the experimental composites (Figure 10).

Garoushi et al. and Petersen [17, 19] showed that glass fibers below the critical length decreased the flexural strength tested specimens. SEM of G7.5 and G17.5 groups showed an homogeneous resin matrix, but with significant lower flexural strength than the control group. Even with lower proportion of GFP in these groups, these fillers could not act as real fillers nor fibers, occupying spaces and creating weaker regions prone to crack propagation, as seen in figures (Figures 5 and 6).

The high concentration of GFP on the remaining groups (G27.5; G37.5 and G47.5) produced a visually dry and heterogeneous resin matrix, which means poor interaction with fibers and fillers. It was also observed the presence of large clusters of GFP jeopardizing the adhesion of reinforcing fibers to the resinous matrix. These were important facts contributing to the decrease in flexural and diametral strength of the composite. The production of a heterogeneous matrix made it difficult to handle during laboratory procedures [22], impairing wetting of reinforcing fibers by the resin matrix. Internal defects or bubbles in a heterogeneous resin matrix can store water, which leads to its degradation [44].

The percentage increase in load by weight of fillers within a composite resin tends to increase its surface hardness [35]. The present study did not changed the total amount of fillers within the experimental composite but varied the proportion and type of fillers. Then it was not expected, at this point of view, differences in Knoop microhardness measurements. However, since GFP did not act as real fillers, Knoop microhardness decreased in all groups, except G37.5, in comparison to the control group.

The control group SEM analysis (Figure 4) showed a homogeneous matrix adhered to reinforcing fibers, without the presence of cracks or bubbles, which ensured greater mechanical strength for the composite [11, 14, 22]. In the control group the presence of short silanized reinforcing fibers within the critical fiber length enabled better interaction of the fibers with the resin matrix resin, reducing weakness areas [42, 43].

The present study certified the importance of filler distribution and interaction with resin matrix on mechanical strength of an experimental fiber reinforced composite. However it was not possible to use glass fibers and filler particles after

milling procedures, which could enable better results. Further studies should improve the method of fiber milling in order to produce a powder with smaller particle sizes or make a better surface treatment which can increase its interaction with the resin matrix.

## 5 CONCLUSION

Within the obtained results and according to the employed methods, it is possible to conclude that:

- a) Gradual replacement of barium silicate by fiber glass powder in a fiber reinforced experimental resin showed reduction of flexural and diametral tensile strength, and Knoop microhardness.
- b) Filler size of glass fiber powder (higher than barium silicate and lower than critical fiber length) was the main reason for obtained results.
- c) The interactions of GFP fillers with the resin matrix and fiber reinforcement were negative.

## 6 REFERENCES

1. Atai, M., A. Pahlavan, and N. Moin, *Nano-porous thermally sintered nano silica as novel fillers for dental composites*. Dent Mater, 2012. **28**(2): p. 133-45.
2. Ellakwa, A.E., A.C. Shortall, and P.M. Marquis, *Influence of fiber type and wetting agent on the flexural properties of an indirect fiber reinforced composite*. J Prosthet Dent, 2002. **88**(5): p. 485-90.
3. Dyer, S.R., et al., *Effect of cross-sectional design on the modulus of elasticity and toughness of fiber-reinforced composite materials*. J Prosthet Dent, 2005. **94**(3): p. 219-26.
4. Garoushi, S., P.K. Vallittu, and L.V. Lassila, *Fracture resistance of short, randomly oriented, glass fiber-reinforced composite premolar crowns*. Acta Biomater, 2007. **3**(5): p. 779-84.
5. Dyer, S.R., et al., *Damage mechanics and load failure of fiber-reinforced composite fixed partial dentures*. Dent Mater, 2005. **21**(12): p. 1104-10.
6. Garoushi, S., P.K. Vallittu, and L.V. Lassila, *Continuous and short fiber reinforced composite in root post-core system of severely damaged incisors*. Open Dent J, 2009. **3**: p. 36-41.
7. Garoushi, S., P.K. Vallittu, and L.V. Lassila, *Use of short fiber-reinforced composite with semi-interpenetrating polymer network matrix in fixed partial dentures*. J Dent, 2007. **35**(5): p. 403-8.
8. Bertassoni, L.E., et al., *Effect of pre- and postpolymerization on flexural strength and elastic modulus of impregnated, fiber-reinforced denture base acrylic resins*. J Prosthet Dent, 2008. **100**(6): p. 449-57.
9. Garoushi, S.K., et al., *Fiber-reinforced onlay composite resin restoration: a case report*. J Contemp Dent Pract, 2009. **10**(4): p. 104-10.
10. Venhoven, B.A., et al., *Influence of filler parameters on the mechanical coherence of dental restorative resin composites*. Biomaterials, 1996. **17**(7): p. 735-40.
11. Taylor, D.F., et al., *Relationship between filler and matrix resin characteristics and the properties of uncured composite pastes*. Biomaterials, 1998. **19**(1-3): p. 197-204.
12. Lassila, L.V. and P.K. Vallittu, *The effect of fiber position and polymerization condition on the flexural properties of fiber-reinforced composite*. J Contemp Dent Pract, 2004. **5**(2): p. 14-26.
13. Dyer, S.R., et al., *Effect of fiber position and orientation on fracture load of fiber-reinforced composite*. Dent Mater, 2004. **20**(10): p. 947-55.
14. Cekic-Nagas, I., et al., *Effect of fiber-reinforced composite at the interface on bonding of resin core system to dentin*. Dent Mater J, 2008. **27**(5): p. 736-43.
15. Kumbuloglu, O., M. Ozcan, and A. User, *Fracture strength of direct surface-retained fixed partial dentures: effect of fiber reinforcement versus the use of particulate filler composites only*. Dent Mater J, 2008. **27**(2): p. 195-202.
16. Garoushi, S., et al., *Load bearing capacity of fibre-reinforced and particulate filler composite resin combination*. J Dent, 2006. **34**(3): p. 179-84.
17. Garoushi, S., L.V. Lassila, and P.K. Vallittu, *The effect of span length of flexural testing on properties of short fiber reinforced composite*. J Mater Sci Mater Med, 2012. **23**(2): p. 325-8.



18. Callaghan, D.J., A. Vaziri, and H. Nayeb-Hashemi, *Effect of fiber volume fraction and length on the wear characteristics of glass fiber-reinforced dental composites*. Dent Mater, 2006. **22**(1): p. 84-93.
19. Petersen, R.C., *Discontinuous fiber-reinforced composites above critical length*. J Dent Res, 2005. **84**(4): p. 365-70.
20. Garoushi, S.K., L.V. Lassila, and P.K. Vallittu, *Short fiber reinforced composite: the effect of fiber length and volume fraction*. J Contemp Dent Pract, 2006. **7**(5): p. 10-7.
21. Obukuro, M., Y. Takahashi, and H. Shimizu, *Effect of diameter of glass fibers on flexural properties of fiber-reinforced composites*. Dent Mater J, 2008. **27**(4): p. 541-8.
22. Lastumaki, T.M., L.V. Lassila, and P.K. Vallittu, *The semi-interpenetrating polymer network matrix of fiber-reinforced composite and its effect on the surface adhesive properties*. J Mater Sci Mater Med, 2003. **14**(9): p. 803-9.
23. Fonseca, R.B., et al., *Reinforcement of Dental Methacrylate with Glass Fiber after Heated Silane Application*. BioMed Research International, 2014. **2014**: p. 5.
24. Garoushi, S., P.K. Vallittu, and L.V. Lassila, *Short glass fiber reinforced restorative composite resin with semi-inter penetrating polymer network matrix*. Dent Mater, 2007. **23**(11): p. 1356-62.
25. Kim, K.H., J.L. Ong, and O. Okuno, *The effect of filler loading and morphology on the mechanical properties of contemporary composites*. J Prosthet Dent, 2002. **87**(6): p. 642-9.
26. Sabbagh, J., et al., *Characterization of the inorganic fraction of resin composites*. J Oral Rehabil, 2004. **31**(11): p. 1090-101.
27. Adabo, G.L., et al., *The volumetric fraction of inorganic particles and the flexural strength of composites for posterior teeth*. J Dent, 2003. **31**(5): p. 353-9.
28. Chen, L., et al., *BisGMA/TEGDMA dental composite containing high aspect-ratio hydroxyapatite nanofibers*. Dent Mater, 2011. **27**(11): p. 1187-95.
29. Garoushi, S., L.V. Lassila, and P.K. Vallittu, *Influence of nanometer scale particulate fillers on some properties of microfilled composite resin*. J Mater Sci Mater Med, 2011. **22**(7): p. 1645-51.
30. Ikejima, I., R. Nomoto, and J.F. McCabe, *Shear punch strength and flexural strength of model composites with varying filler volume fraction, particle size and silanation*. Dent Mater, 2003. **19**(3): p. 206-11.
31. Karabela, M.M. and I.D. Sideridou, *Synthesis and study of properties of dental resin composites with different nanosilica particles size*. Dent Mater, 2011. **27**(8): p. 825-35.
32. Kondo, Y., et al., *Effect of PMMA filler particles addition on the physical properties of resin composite*. Dent Mater J, 2010. **29**(5): p. 596-601.
33. Rastelli, A.N., et al., *The filler content of the dental composite resins and their influence on different properties*. Microsc Res Tech, 2012. **75**(6): p. 758-65.
34. Ruddell, D.E., M.M. Maloney, and J.Y. Thompson, *Effect of novel filler particles on the mechanical and wear properties of dental composites*. Dent Mater, 2002. **18**(1): p. 72-80.
35. Beun, S., et al., *Characterization of nanofilled compared to universal and microfilled composites*. Dent Mater, 2007. **23**(1): p. 51-9.

36. Curtis, A.R., et al., *The mechanical properties of nanofilled resin-based composites: characterizing discrete filler particles and agglomerates using a micromanipulation technique*. Dent Mater, 2009. **25**(2): p. 180-7.
37. Mortazavi, V., et al., *The effect of nanoclay filler loading on the flexural strength of fiber-reinforced composites*. Dent Res J (Isfahan), 2012. **9**(3): p. 273-80.
38. Association, A.D., *Resin-based filling materials*, in ADA Standard No. 27. 1993: Chicago, IL.
39. 4049, I., *Polymer based filling, restorative and luting materials*, in Organization IS. 2000.
40. Lassila, L.V., et al., *Evaluation of some properties of two fiber-reinforced composite materials*. Acta Odontol Scand, 2005. **63**(4): p. 196-204.
41. Abdulmajeed, A.A., et al., *The effect of high fiber fraction on some mechanical properties of unidirectional glass fiber-reinforced composite*. Dent Mater, 2011. **27**(4): p. 313-21.
42. Frese, C., et al., *Original and repair bond strength of fiber-reinforced composites in vitro*. Dent Mater, 2014. **30**(4): p. 456-62.
43. Garoushi, S., et al., *Polymerization shrinkage of experimental short glass fiber-reinforced composite with semi-inter penetrating polymer network matrix*. Dent Mater, 2008. **24**(2): p. 211-5.
44. Lassila, L.V., T. Nohrstrom, and P.K. Vallittu, *The influence of short-term water storage on the flexural properties of unidirectional glass fiber-reinforced composites*. Biomaterials, 2002. **23**(10): p. 2221-9.

#### 4 CONSIDERAÇÕES FINAIS

a) A substituição gradativa em percentual do silicato de bário pelo pó de fibra de vidro em uma resina experimental reforçada com fibra de vidro curta de 3 mm não apresentou melhoria nos testes de resistência flexural e diametral.

b) Morfologicamente a partícula do pó de fibra de vidro apresentou-se heterogênea e maior que a partícula do silicato de bário.

c) As interações da partícula do pó de fibra de vidro com a matriz resinosa e o reforço de fibra foram negativos.

## 5 REFERÊNCIAS

1. Atai, M., A. Pahlavan, and N. Moin, *Nano-porous thermally sintered nano silica as novel fillers for dental composites*. Dent Mater, 2012. **28**(2): p. 133-45.
2. Ellakwa, A.E., A.C. Shortall, and P.M. Marquis, *Influence of fiber type and wetting agent on the flexural properties of an indirect fiber reinforced composite*. J Prosthet Dent, 2002. **88**(5): p. 485-90.
3. Dyer, S.R., et al., *Effect of cross-sectional design on the modulus of elasticity and toughness of fiber-reinforced composite materials*. J Prosthet Dent, 2005. **94**(3): p. 219-26.
4. Garoushi, S., P.K. Vallittu, and L.V. Lassila, *Fracture resistance of short, randomly oriented, glass fiber-reinforced composite premolar crowns*. Acta Biomater, 2007. **3**(5): p. 779-84.
5. Dyer, S.R., et al., *Damage mechanics and load failure of fiber-reinforced composite fixed partial dentures*. Dent Mater, 2005. **21**(12): p. 1104-10.
6. Garoushi, S., P.K. Vallittu, and L.V. Lassila, *Continuous and short fiber reinforced composite in root post-core system of severely damaged incisors*. Open Dent J, 2009. **3**: p. 36-41.
7. Garoushi, S., P.K. Vallittu, and L.V. Lassila, *Use of short fiber-reinforced composite with semi-interpenetrating polymer network matrix in fixed partial dentures*. J Dent, 2007. **35**(5): p. 403-8.
8. Bertassoni, L.E., et al., *Effect of pre- and postpolymerization on flexural strength and elastic modulus of impregnated, fiber-reinforced denture base acrylic resins*. J Prosthet Dent, 2008. **100**(6): p. 449-57.
9. Garoushi, S.K., et al., *Fiber-reinforced onlay composite resin restoration: a case report*. J Contemp Dent Pract, 2009. **10**(4): p. 104-10.
10. Venhoven, B.A., et al., *Influence of filler parameters on the mechanical coherence of dental restorative resin composites*. Biomaterials, 1996. **17**(7): p. 735-40.
11. Taylor, D.F., et al., *Relationship between filler and matrix resin characteristics and the properties of uncured composite pastes*. Biomaterials, 1998. **19**(1-3): p. 197-204.
12. Lassila, L.V. and P.K. Vallittu, *The effect of fiber position and polymerization condition on the flexural properties of fiber-reinforced composite*. J Contemp Dent Pract, 2004. **5**(2): p. 14-26.
13. Dyer, S.R., et al., *Effect of fiber position and orientation on fracture load of fiber-reinforced composite*. Dent Mater, 2004. **20**(10): p. 947-55.
14. Cekic-Nagas, I., et al., *Effect of fiber-reinforced composite at the interface on bonding of resin core system to dentin*. Dent Mater J, 2008. **27**(5): p. 736-43.
15. Kumbuloglu, O., M. Ozcan, and A. User, *Fracture strength of direct surface-retained fixed partial dentures: effect of fiber reinforcement versus the use of particulate filler composites only*. Dent Mater J, 2008. **27**(2): p. 195-202.
16. Garoushi, S., et al., *Load bearing capacity of fibre-reinforced and particulate filler composite resin combination*. J Dent, 2006. **34**(3): p. 179-84.
17. Garoushi, S., L.V. Lassila, and P.K. Vallittu, *The effect of span length of flexural testing on properties of short fiber reinforced composite*. J Mater Sci Mater Med, 2012. **23**(2): p. 325-8.

18. Callaghan, D.J., A. Vaziri, and H. Nayeb-Hashemi, *Effect of fiber volume fraction and length on the wear characteristics of glass fiber-reinforced dental composites*. Dent Mater, 2006. **22**(1): p. 84-93.
19. Petersen, R.C., *Discontinuous fiber-reinforced composites above critical length*. J Dent Res, 2005. **84**(4): p. 365-70.
20. Garoushi, S.K., L.V. Lassila, and P.K. Vallittu, *Short fiber reinforced composite: the effect of fiber length and volume fraction*. J Contemp Dent Pract, 2006. **7**(5): p. 10-7.
21. Obukuro, M., Y. Takahashi, and H. Shimizu, *Effect of diameter of glass fibers on flexural properties of fiber-reinforced composites*. Dent Mater J, 2008. **27**(4): p. 541-8.
22. Lastumaki, T.M., L.V. Lassila, and P.K. Vallittu, *The semi-interpenetrating polymer network matrix of fiber-reinforced composite and its effect on the surface adhesive properties*. J Mater Sci Mater Med, 2003. **14**(9): p. 803-9.
23. Fonseca, R.B., et al., *Reinforcement of Dental Methacrylate with Glass Fiber after Heated Silane Application*. BioMed Research International, 2014. **2014**: p. 5.
24. Garoushi, S., P.K. Vallittu, and L.V. Lassila, *Short glass fiber reinforced restorative composite resin with semi-inter penetrating polymer network matrix*. Dent Mater, 2007. **23**(11): p. 1356-62.
25. Kim, K.H., J.L. Ong, and O. Okuno, *The effect of filler loading and morphology on the mechanical properties of contemporary composites*. J Prosthet Dent, 2002. **87**(6): p. 642-9.
26. Sabbagh, J., et al., *Characterization of the inorganic fraction of resin composites*. J Oral Rehabil, 2004. **31**(11): p. 1090-101.
27. Adabo, G.L., et al., *The volumetric fraction of inorganic particles and the flexural strength of composites for posterior teeth*. J Dent, 2003. **31**(5): p. 353-9.
28. Chen, L., et al., *BisGMA/TEGDMA dental composite containing high aspect-ratio hydroxyapatite nanofibers*. Dent Mater, 2011. **27**(11): p. 1187-95.
29. Garoushi, S., L.V. Lassila, and P.K. Vallittu, *Influence of nanometer scale particulate fillers on some properties of microfilled composite resin*. J Mater Sci Mater Med, 2011. **22**(7): p. 1645-51.
30. Ikejima, I., R. Nomoto, and J.F. McCabe, *Shear punch strength and flexural strength of model composites with varying filler volume fraction, particle size and silanation*. Dent Mater, 2003. **19**(3): p. 206-11.
31. Karabela, M.M. and I.D. Sideridou, *Synthesis and study of properties of dental resin composites with different nanosilica particles size*. Dent Mater, 2011. **27**(8): p. 825-35.
32. Kondo, Y., et al., *Effect of PMMA filler particles addition on the physical properties of resin composite*. Dent Mater J, 2010. **29**(5): p. 596-601.
33. Rastelli, A.N., et al., *The filler content of the dental composite resins and their influence on different properties*. Microsc Res Tech, 2012. **75**(6): p. 758-65.
34. Ruddell, D.E., M.M. Maloney, and J.Y. Thompson, *Effect of novel filler particles on the mechanical and wear properties of dental composites*. Dent Mater, 2002. **18**(1): p. 72-80.
35. Beun, S., et al., *Characterization of nanofilled compared to universal and microfilled composites*. Dent Mater, 2007. **23**(1): p. 51-9.

36. Curtis, A.R., et al., *The mechanical properties of nanofilled resin-based composites: characterizing discrete filler particles and agglomerates using a micromanipulation technique*. Dent Mater, 2009. **25**(2): p. 180-7.
37. Mortazavi, V., et al., *The effect of nanoclay filler loading on the flexural strength of fiber-reinforced composites*. Dent Res J (Isfahan), 2012. **9**(3): p. 273-80.
38. Association, A.D., *Resin-based filling materials*, in ADA Standard No. 27. 1993: Chicago, IL.
39. 4049, I., *Polymer based filling, restorative and luting materials*, in Organization IS. 2000.
40. Lassila, L.V., et al., *Evaluation of some properties of two fiber-reinforced composite materials*. Acta Odontol Scand, 2005. **63**(4): p. 196-204.
41. Abdulmajeed, A.A., et al., *The effect of high fiber fraction on some mechanical properties of unidirectional glass fiber-reinforced composite*. Dent Mater, 2011. **27**(4): p. 313-21.
42. Frese, C., et al., *Original and repair bond strength of fiber-reinforced composites in vitro*. Dent Mater, 2014. **30**(4): p. 456-62.
43. Garoushi, S., et al., *Polymerization shrinkage of experimental short glass fiber-reinforced composite with semi-inter penetrating polymer network matrix*. Dent Mater, 2008. **24**(2): p. 211-5.
44. Lassila, L.V., T. Nohrstrom, and P.K. Vallittu, *The influence of short-term water storage on the flexural properties of unidirectional glass fiber-reinforced composites*. Biomaterials, 2002. **23**(10): p. 2221-9.

## 6 ANEXOS

## ANEXO A

Tabela 1. Grupos Experimentais

GROUPS	PROPORTIONS			
	% short glass fiber 3mm	% Resin	% Particle loading (barium silicate)	% Particle loading (powdered glass fiber)
CONTROL	30	22.5	47.5	0.0
G7.5	30	22.5	40.0	7.5
G17.5	30	22.5	30.0	17.5
G27.5	30	22.5	20.0	27.5
G37.5	30	22.5	10.0	37.5
G47.5	30	22.5	0.0	47.5

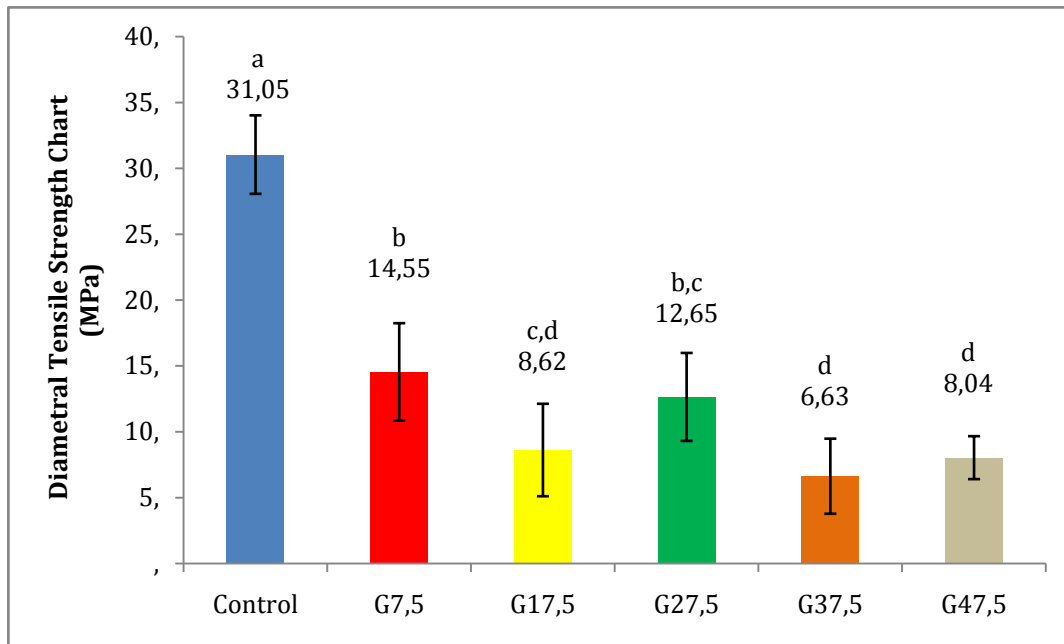


Figure 1. Diametral Tensile Strength Chart (MPa) - The graph shows the average resistance to diametral strength of the experimental groups. Same letters show that there was no statistical difference between the experimental groups, with  $p > 0.05$ .



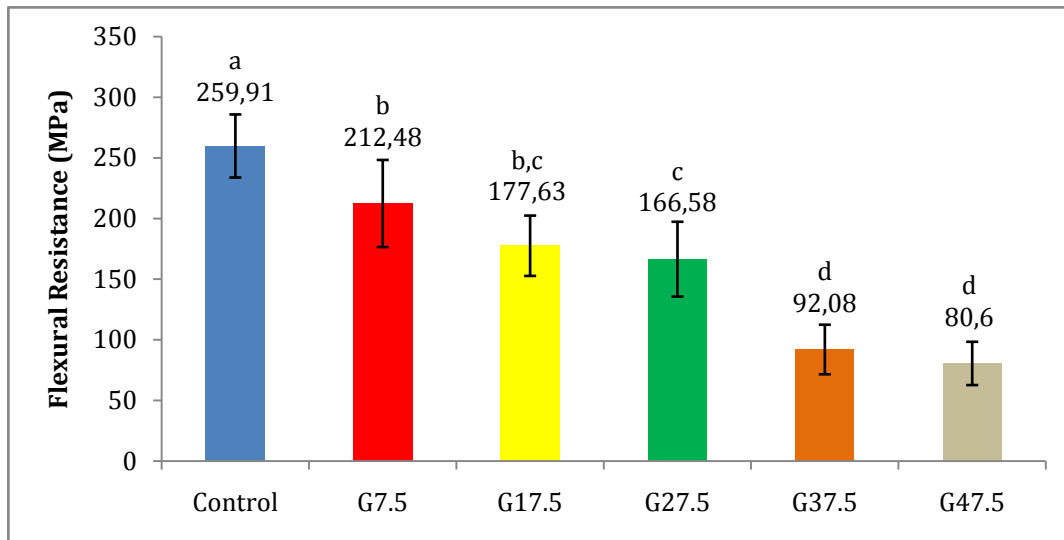


Figure 2. Flexural Resistance Chart (MPa). The graph shows the average flexural strength of the experimental groups. Same letters show that there was no statistical difference between the experimental groups, with  $p > 0.05$ .

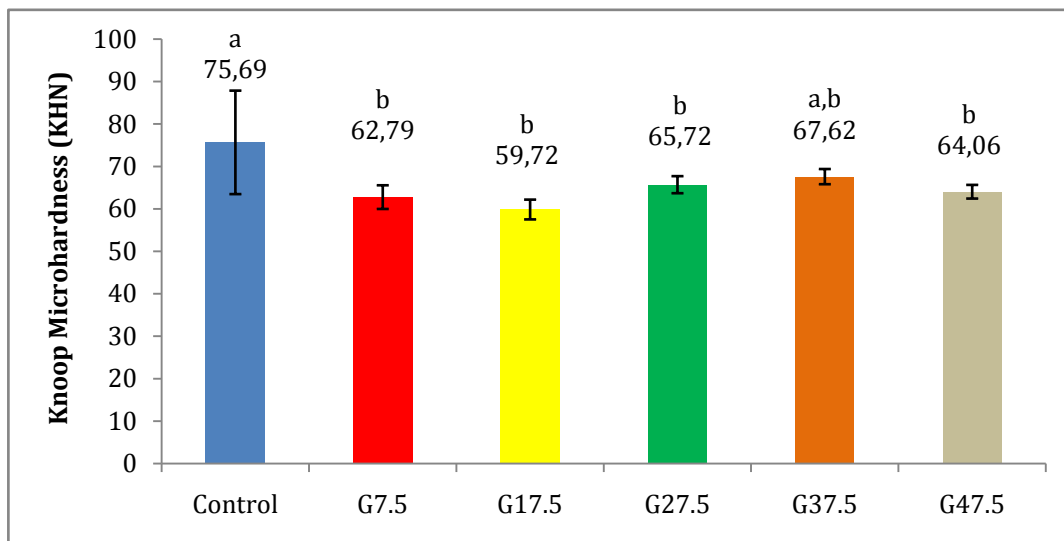


Figure 3. Microhardness Knoop Graph (KHN). The graph shows the average knoop hardness of the experimental groups. Same letters show that there was no statistical difference between the experimental groups, with  $p > 0.05$ .

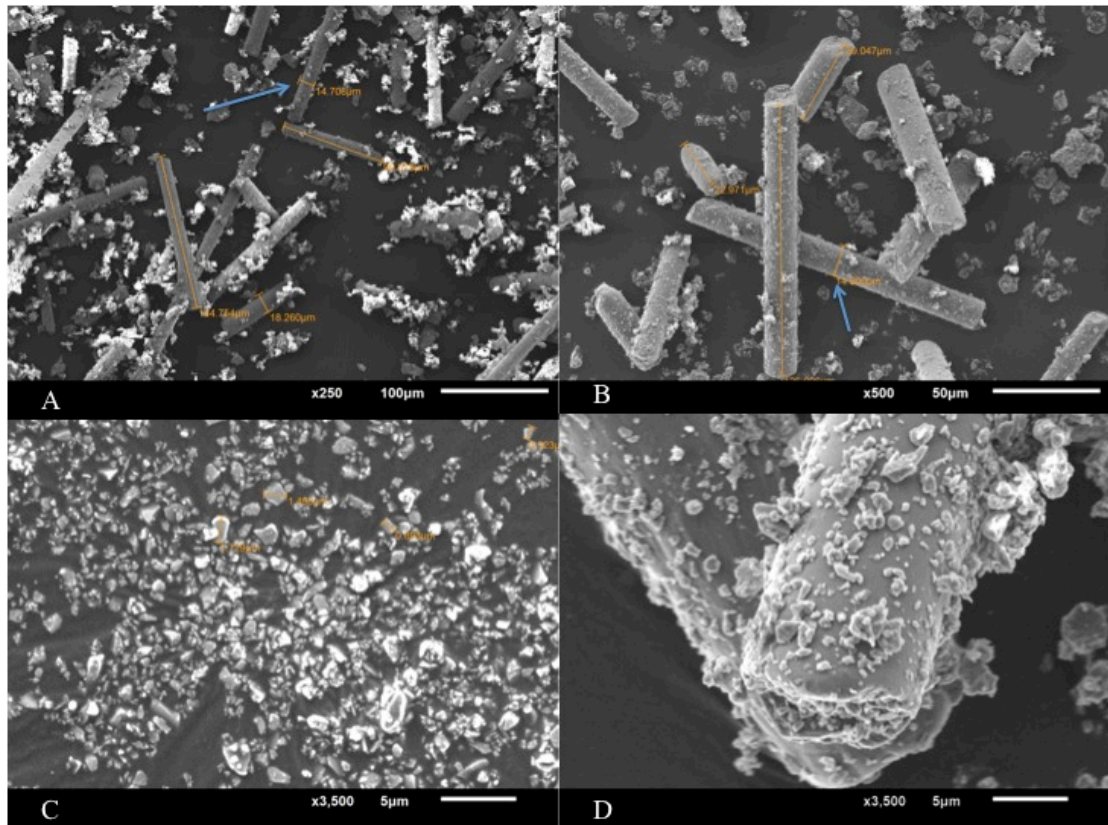


Figure 4. Scanning Electron Microscopy - Cargo particles: A - fiberglass powder with an increase of 250 x; B - glass fiber powder magnified 500 x; C - barium silicate with an increase of 3500 x; D - barium silicate glass fibers adhered to an increase of 3500 x.

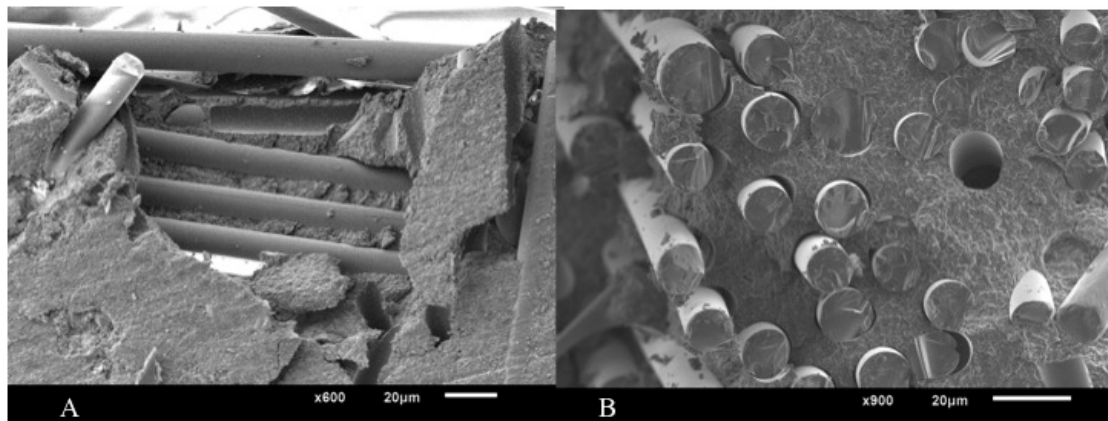
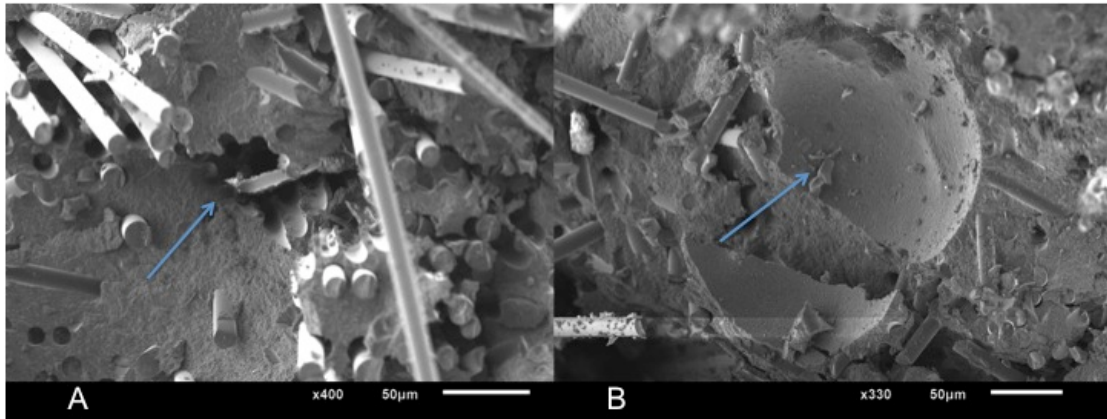
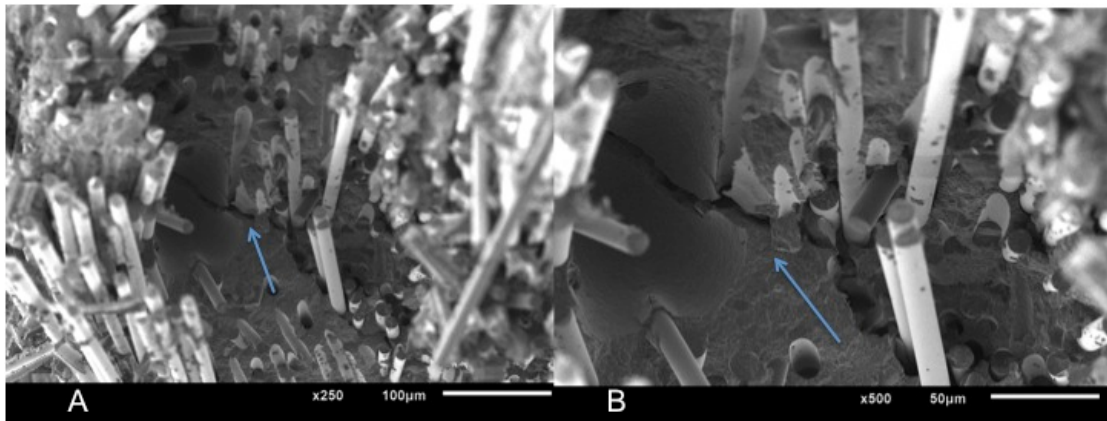


Figure 5. Scanning Electron Microscopy - Group CONTROL: A - Fiberglass resin matrix adhered to an increase of 600 x; B - resinous matrix with homogeneous appearance with an increase of 900 x.



**Figure 6. Scanning Electron Microscopy of G7.5 Group. A - crack presence and absence of reinforcing fiber in the crack region (see arrow), an increase of 400 x. B - Presence bubble with reinforcing fiber in the absence of the bubble region increase in 330x.**



**Figure 7. Scanning Electron Microscopy of G17.5 Group. Association A- crack and blister of a reinforcing fiber absence region 250 x increases. B - Same region with an increase of 500 x.**

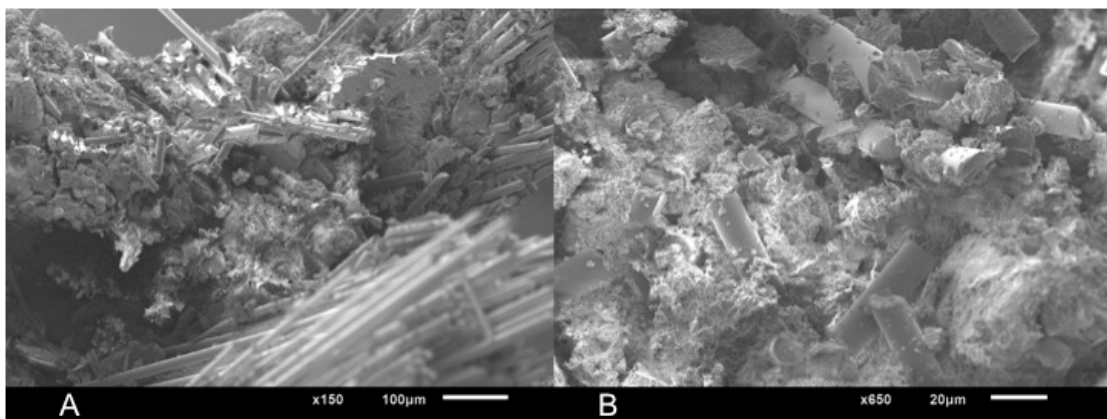


**Figure 8. Scanning Electron Microscopy of G27.5 Group. A - resin matrix heterogeneous groups with single glass fiber powder, an increase of 150 x. B - Same region with an increase in 650 x, the beam multidirectional glass fiber powder.**

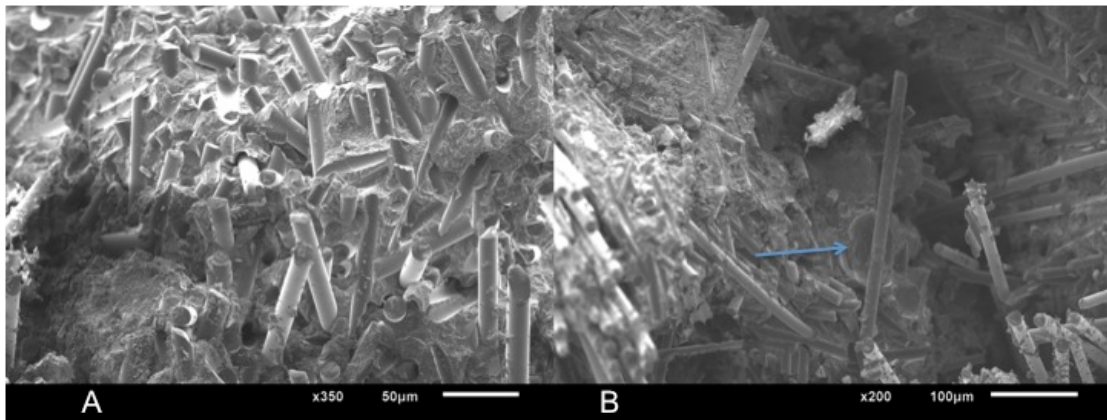


Figure 9. Scanning Electron Microscopy of G37.5 Group. A - Particleboard multidirectional glass fiber bundles powder and no reinforcing fiber, up to 350 x. B - Area with a 200 x, bulla and heterogeneous matrix and no reinforcing fiber.

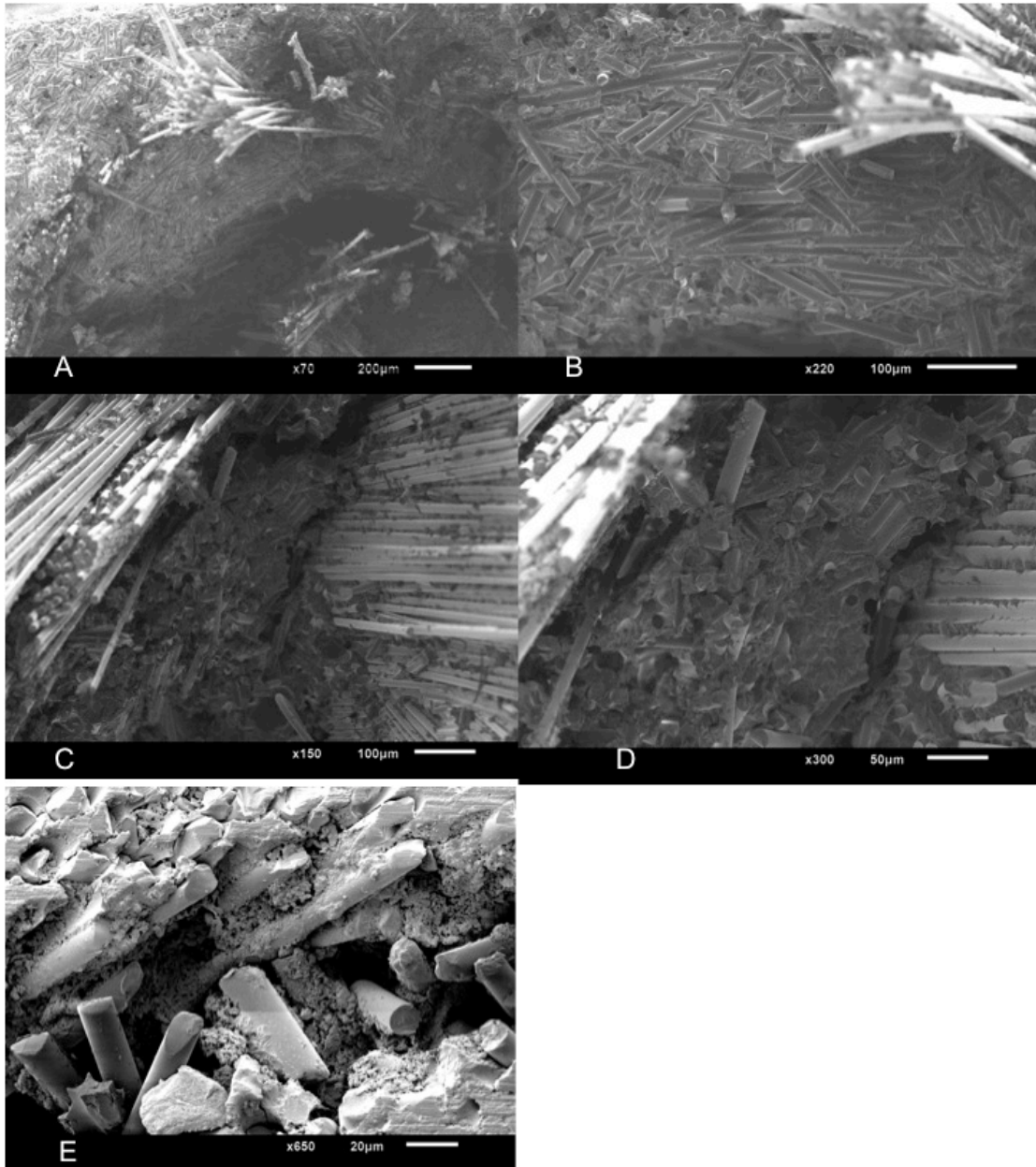


Figure 10. Scanning Electron Microscopy of G47.5 Group. A and B - Agglomerates glass fiber powder, reinforcing fibers sequence with increases of 150 x 350 x the same region. C and D - interspersed with reinforcing fibers, glass fiber powder agglomerates with increases in sequence of 150 x 350 x the same region. E - bit resin matrix adhered to glass fiber powder, an increase of 650 x.

## ANEXO B

# JMR Instructions - Format

[Style](#) | [Mathematics](#) | [References](#) | [Tables](#) | [Acknowledgements](#) | [Rights and Permissions](#) | [Proofs of Articles](#)

## Style

Authors are expected to follow the conventional writing, notation, and illustration style prescribed in 1) *The ACS Style Guide*, 3<sup>rd</sup> Edition, 2006 or 2) *Scientific Style and Format*, the *CSE Manual for Authors, Editors and Publishers*, 7th edition, 2006. Authors should also study the form and style of printed material in this journal. SI units should be used. Authors should use an identical format for their names in all publications to facilitate use of citations and author indexes.

## Mathematics

Special care should be given to make equations and formulas clear to the typesetter.

*Variables* should appear in italic text.

**Vectors** should appear in bold text.

Capital and lower-case letters should be distinguished clearly where there could be confusion.

Fractional exponents should be used to avoid root signs.

Extra symbols should be introduced to avoid complicated exponents or where it is necessary to repeat a complicated expression a number of times.

The slash (/) should be used wherever possible for fractions.

Mathematical derivations that are easily found elsewhere in the literature should not be used.

## References

All journal article references must include the title of the article and all authors. The phrases et al. and ibid. should not be used in any reference. Instead, all authors of the reference should be listed. All journal article references must include the initials and last name of all authors: the title of the article in italic, the volume number in bold, page number and (year).

Authors are responsible for providing English-language translations of reference

citations originally published in other languages.

References should be double-spaced, numbered consecutively, placed on a separate page, and arranged thus:

1. A. Gouldstone, Y-L. Shen, S. Suresh, and C.V. Thompson: Evolution of stress in passivated and unpassivated metal interconnects. *J. Mater. Res.* **13**, 1956 (1998).
2. H. Lamb: Hydrodynamics, 6th ed. (Cambridge Univ. Press, Cambridge, England, 1940), pp. 573, 645.
3. T.R. Jervis, J-P. Hirvonen, M. Nastasi, and M.R. Cohen: Laser mixing of titanium on silicon carbide, in Beam-Solid Interactions: Physical Phenomena, edited by J.A. Knapp, P. Borgesen, and R.A. Zuhr (Mater. Res. Soc. Symp. Proc. **157**, Pittsburgh, PA, 1990), p. 395.
4. H. Wang, A. Sharma, and A. Kvit: Mechanical properties of nanocrystalline and epitaxial TiN films on (100) silicon. *J. Mater. Res.* **16**, 9 (2001).

Please take note of the reference format for the following MRS publications:

**MRS Communications** T. Yokoto, T. Sekitani, Y. Kato, K. Kuribara, U. Zschieschang, H. Klauk, T. Yamamoto, K. Takimiya, H. Kuwabara, M. Ikeda, and T. Someya: Low-voltage organic transistor with subfemtoliter inkjet source-drain contacts. *MRS Communications*, doi:10.1557/mrc.2011.4, Published online 17 June 2011.

**Journal of Materials Research** G. Bakan, N. Khan, A. Cywar, K. Cil, M. Akbulut, A. Gokirmak, and H. Silva: Self-heating of silicon microwires: Crystallization and thermoelectric effects. *J. Mater. Res.* **26**(9), 1061 (2011).

**MRS Bulletin** B.M. Moskal and L. Kosbar: Addressing broader impacts through K–12 outreach in materials education. *MRS Bull.* **36**(4), 255 (2011).

**MRS Symposium Proceedings** Print volume: T.R. Jervis, J-P. Hirvonen, M. Nastasi, and M.R. Cohen: Laser mixing of titanium on silicon carbide, in Beam-Solid Interactions: Physical Phenomena, edited by J.A. Knapp, P. Borgesen, and R.A. Zuhr (Mater. Res. Soc. Symp. Proc. **157**, Pittsburgh, PA, 1990), p. 395.

Electronic volume: T. Saif, J. Rajagopalan, and A. Tofangchi: The role of mechanical tension in neurons, in *Biological Materials and Structures in Physiologically Extreme Conditions and Disease*, edited by M.J. Buehler, D. Kaplan, C.T. Lim, and J. Spatz (Mater. Res. Soc. Symp. Proc. **1274**, Warrendale, PA, 2010) 1274-QQ01-06.

## Tables

All but the simplest tabular material should be organized into separate tables. Tables

should be numbered with Roman numerals on separate pages at the end of the manuscript. Captions should be sufficiently descriptive to make the data in the table intelligible without referring to the text. Complicated column headings in the body of the table should be avoided. If necessary, symbols that are explained in the caption should be used.

### **Acknowledgments**

An Acknowledgment(s) section is optional. Please note spelling above. Place statements of funding support and disclaimers in the Acknowledgments section, not in footnotes.

### **Rights and Permissions**

All requests to publish material published in *JMR* should be directed to Cambridge University Press. Please visit Cambridge's Rights and Permissions page:

<http://journals.cambridge.org/action/rightsAndPermissions>

### **Proofs of Articles**

Proofs of Articles accepted for publication will be sent to the communicating author for review electronically and must be returned within 48 hours as instructed. A few alterations in proof are unavoidable; however, the proofing stage is not an opportunity to rewrite a manuscript. Excessive changes at this stage cannot be accommodated. If proofs are not returned, the manuscript will be published as it appears in the final accepted version, with necessary corrections in grammar and spelling in compliance with standard American English and accepted Journal style.

## **JMR Instructions - Figures**

[Format](#) | [Resolution](#) | [File Size](#) | [Labels and Appearance](#) | [Captions](#) | [Color](#) | [Figure Display in Abstract](#) | [Supplementary Material](#)

### **Format:**

High-resolution figures must be uploaded during manuscript submission. The preferred format for figure submission is .tif or .eps format. Figures submitted in pdf format must be saved in separate files.



**Resolution:**

Line drawings and graphs must have a resolution of at least 1200 dpi and a minimum width of 3 inches. Photographs and micrographs must have resolution of at least 350 dpi and a minimum width of 3 inches. For all figures the maximum width is 6 inches. Lower-resolution images will not reproduce properly and will not be accepted. The Editorial Office will provide instructions for ftp of electronic figure submission on an as-needed basis.

**File size:**

There is a 60 MB file upload size limit in *JMR* Manuscripts. Please use LZW compression (which does not affect resolution) when saving figure files.

**Labels and appearance:**

Figure numbers are Arabic: 1, 2, 3. Do not use Roman numerals for figures. Figure parts are labeled with letters: (a), (b), (c).

Figure part labels appear lowercase (a), (b), etc., in the lower left corner outside of figure area. Do not include figure labels within the figures. Do not use capital letters. See sample figure below.

Multi-part figures, which should be submitted as one electronic file, should read horizontally rather than vertically. See sample figure below.

All extraneous machine-generated information in SEM and TEM micrographs must be removed prior to submission and professional quality scale markers placed on the figure (see samples)

Presenting x-ray and neutron diffraction patterns:

X-ray or neutron powder diffraction data should be presented with the diffraction peaks identified to the fullest extent possible. For data from materials with known unit cells, the diffraction peaks should be indexed as shown below. For Miller indices with a value of 10 or higher, an underline is used to more clearly indicate that there are two digits in the index.

Note: by convention the Miller indices of the reflection plane  $hkl$ , written without parentheses, represent the diffracted beam from plane ( $hkl$ ). See sample figure below.

For those diffraction patterns where the phases have unknown unit cells, simply labeling the peaks using a legend is acceptable, as illustrated below:

For diffraction data that have been fitted using a model of some kind, the measured XRD pattern must be shown, along with the difference pattern and the diffraction peak locations. The figure caption will identify the measured and difference patterns as well as all of the phase associated with each set of peak location markers.

(see sample of a typical full-pattern or Rietveld fit)

**Captions:**

Every figure must be referred to in the main text in consecutive numerical order. A caption (legend) must be provided for each figure. Captions must be placed on a separate page at the end of the manuscript. If a figure part such as (a) or (b) is referred to in a caption, that figure part must be labeled.

5. Figure captions are numbered FIG. 1, FIG. 2, FIG. 3, etc. Example: FIG. 1. Concentration dependence of the critical indentation depth,  $h_c$ .
6. Labels appear before what they describe. Example: (a) SEM micrograph, (b) TEM micrograph, and (c) XRD micrograph

**Color:**

All figures submitted in color will appear in color online.

Figures may be printed in color at the author's request for an additional charge.

Color figures must be submitted before the paper is accepted for publication, and cannot be received later in the process.

Authors cannot submit two versions of the same figure, one for color and one for black and white; only one version may be submitted.

Authors need to carefully consider the following when submitting figures in color that will be published in color online only: 1) The colors chosen must reproduce effectively and the colors should be distinguishable when printed in black and white; 2) The descriptions of figures in text and captions must be sufficiently clear for both online and print copy. When submitting figures to be in color online only, authors should include the phrase <<color online>> in the figure captions. This is the author's responsibility.

Authors will see these color figures when viewing their author page proofs on screen.

Authors should always print their page proofs in black and white to see how they will appear in print.

Authors will NOT be allowed to submit color figures to replace black and white figures in the page proof stage.

To maximize the probability that figures will be published in color online and also print as good quality black and white or grayscale graphics, authors are encouraged to follow these figure submission guidelines: 1) Submit a color graphic in Tagged Image File Format (.tif); 2) Submit color graphics with a resolution of at least 300 dpi (600 dpi if there is text or line art in the figure); 3) Submit color graphics in CMYK format; 4) Submit figures sized to fit the actual column or page width of the journal so that reduction or enlargement is not necessary; 5) Submit multipart figures in one single electronic file.

**Figure display in abstract:**

Please identify the figure or figure part that best represents your paper for display in the online abstract. A color figure that is visually interesting and tells the reader at a glance what the paper is about is recommended. Please be specific [i.e., Fig. 3(a) or Fig. 3(b)].

### **Supplementary Material:**

*JMR* allows the submission of supplemental material for online publication. Supplementary Material is defined as any content that supports, but is not key to, the understanding of a published item's message. Given that Supplementary Material is exclusively published online, it may include file types (video, audio) that are incompatible with a print format.

Supplementary Material is subject to the same peer review process and copyright requirements as all primary content. It will be neither copy-edited nor typeset, but will be published as approved by the Editor-in-Chief. Common types of Supplementary Material include audio and video files and large datasets or tables. Datasets, tables, and other textual material are commonly submitted as PDF, Excel, or Word files. The author should ensure that an in-text citation to each Supplementary file has been made in the article. Preferably, in-text citations will appear in a separate section at the end of the article, following the text and preceding the traditional "References" or "Notes" section. Supplementary figures and tables should be labeled as FIG. S1, FIG. S2., etc. and TABLE SI, TABLE SII, etc.

The author will be able to check in page proofs to be certain that the in-text citation appears properly; however, the Supplementary Material files themselves will not be circulated with the page proofs. When an article is published online, either as a FirstView article or as part of an issue, the Supplementary Material will be published online with the article.

Files should be in final, publishable format upon submission. *JMR* will not edit or typeset Supplementary Material, nor will it modify audio or video files in any substantive way. The author will be notified if a submitted file does not meet quality and size requirements.

Some Supplementary Material may not be able to be submitted through our online peer review systems, due to file size or compatibility problems. In such cases, and for all other questions regarding supplementary material, contact the *JMR* Editorial Office.